Untangling the dynamics of the 2019 Ridgecrest sequence by integrated dynamic rupture and Coulomb stress modeling across an immature 3D conjugate fault network

Alice-Agnes Gabriel (LMU Munich)

Taufiqurrahman, Sara Carena, Thomas Ulrich, Duo Li, Bo Li, Aniko Wirp, Alessandro Verdecchia (McGill) & Frantisek Gallovic (CUPrague)

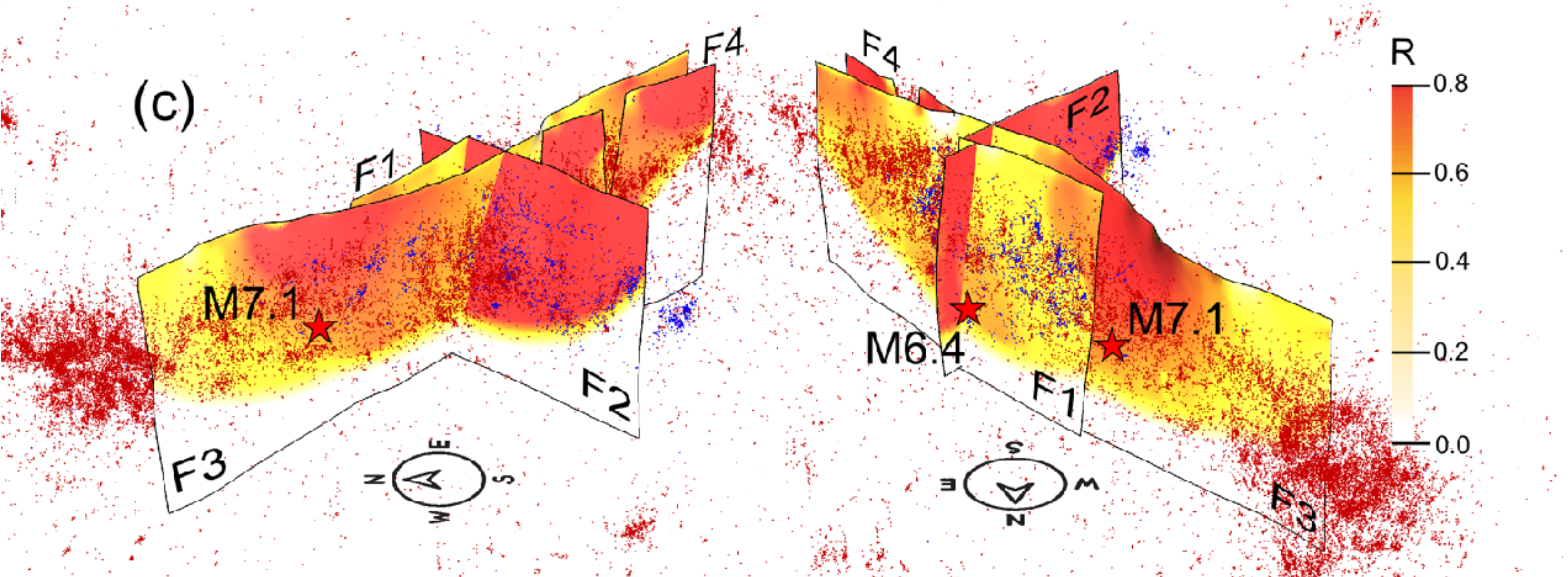

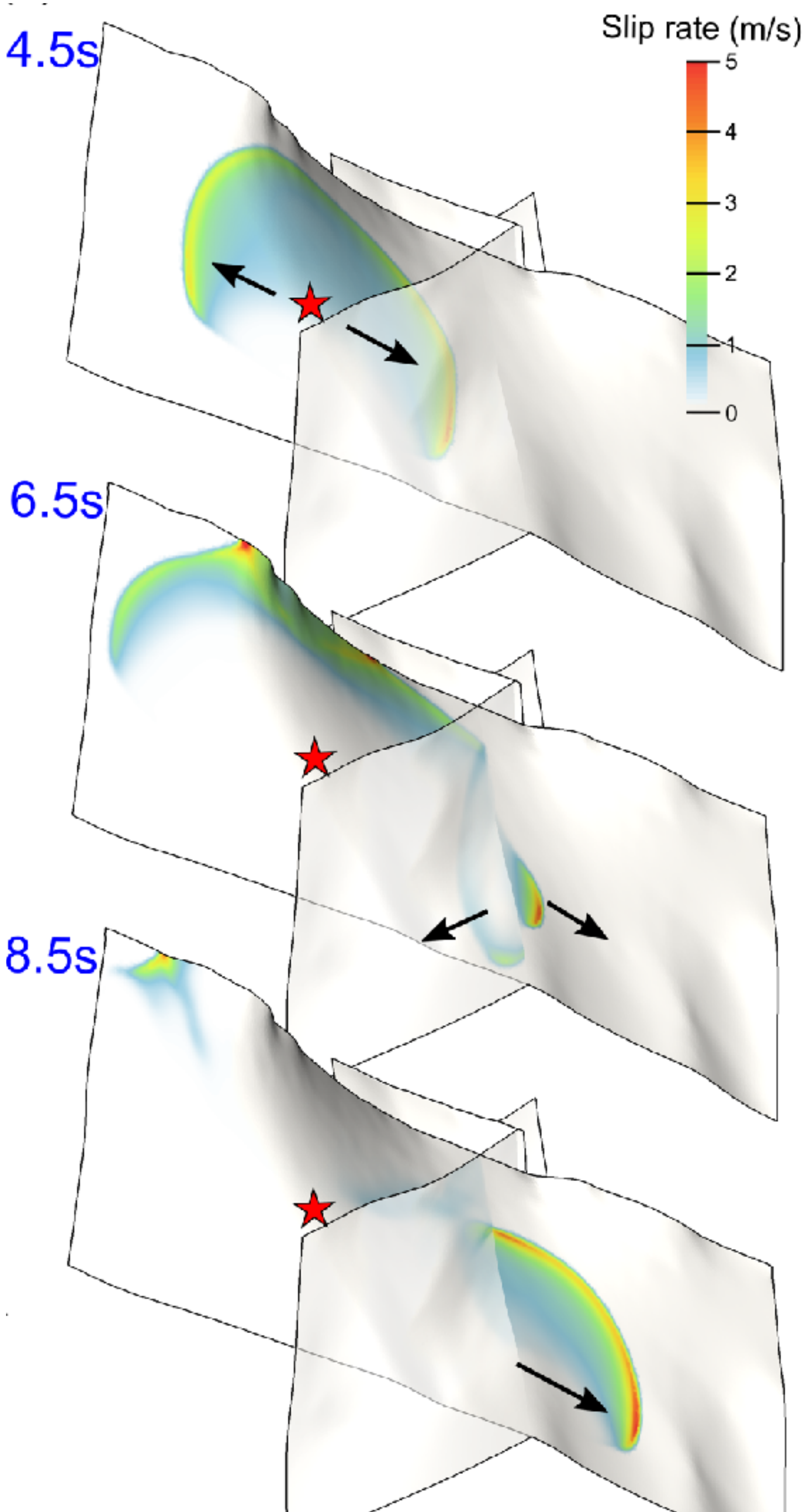

Earthquake source dynamics

Well-recorded earthquakes, as the 2019 M6.4 and M7.1 Ridgecrest sequence, reveal a **striking variability in earthquake source dynamics**

- Multi-fault, hierarchical interlocked orthogonal ruptures challenging seismic hazard practices (Ross et al. 2019)

- Cascading, compound ruptures with variability of rupture styles (cracks and pulses, Chen et al. 2019)

- Dynamic and static fault interaction may have confined events and driven aftershocks/ creep on the Garlock Fault (Lozos and Harris, 2020; Barnhart et al., 2020, Ramos et al., 2020)

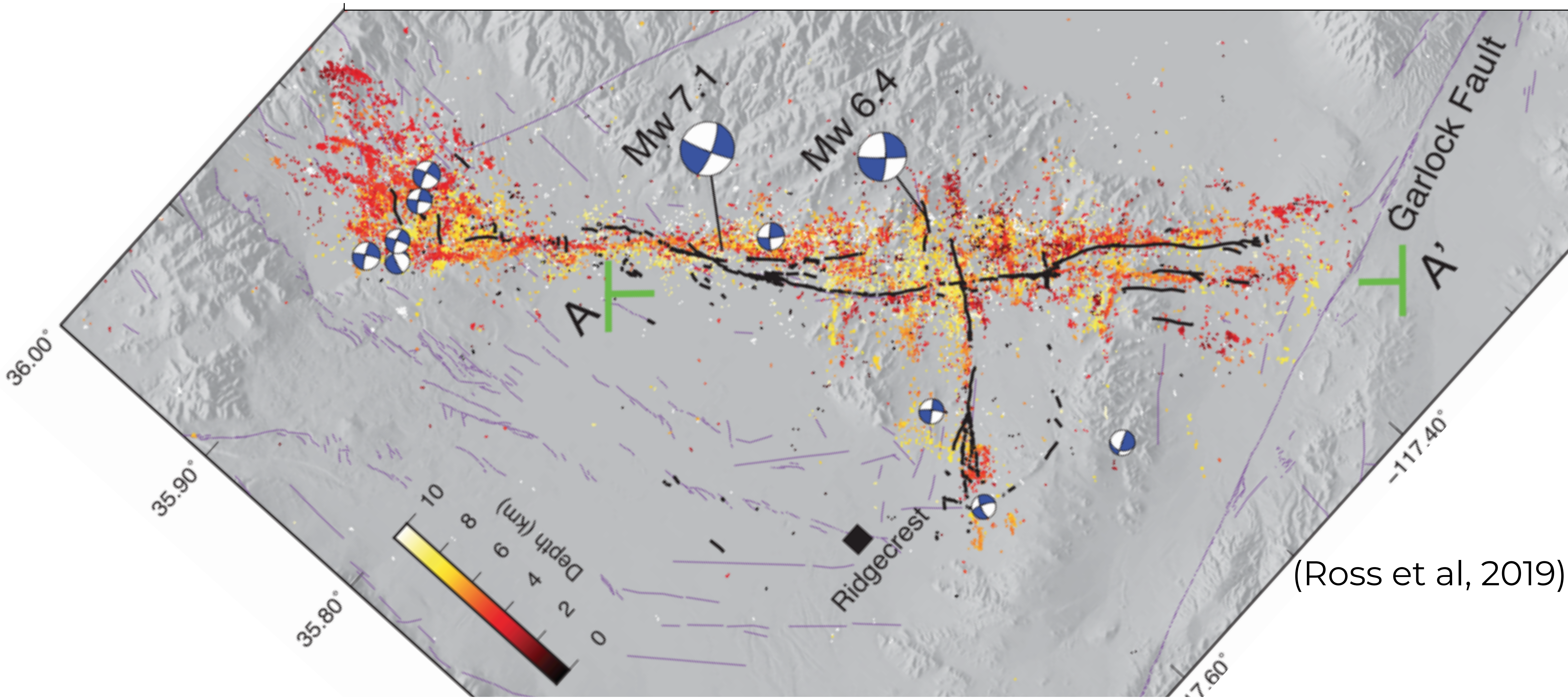

(Ross et al, 2019)

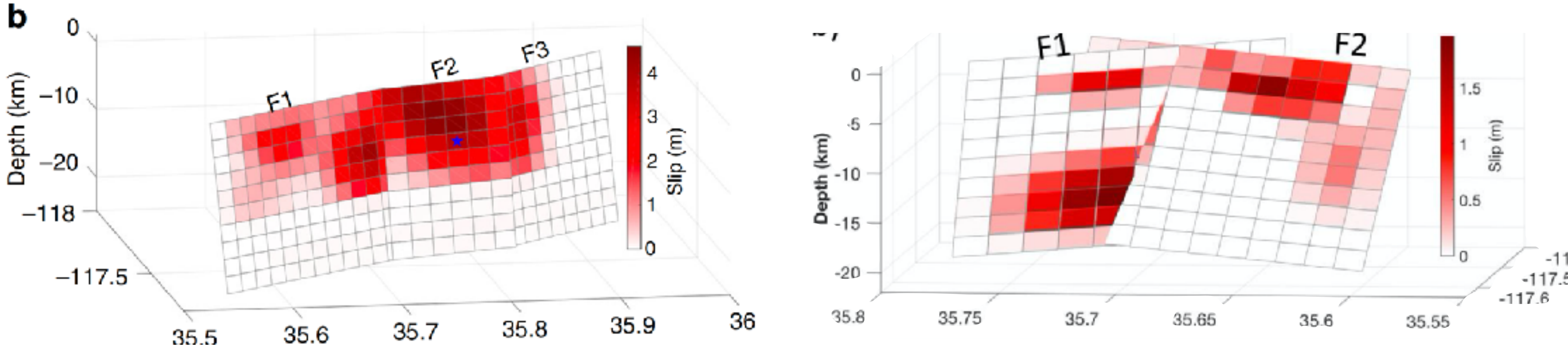

(Chen et al, 2019)

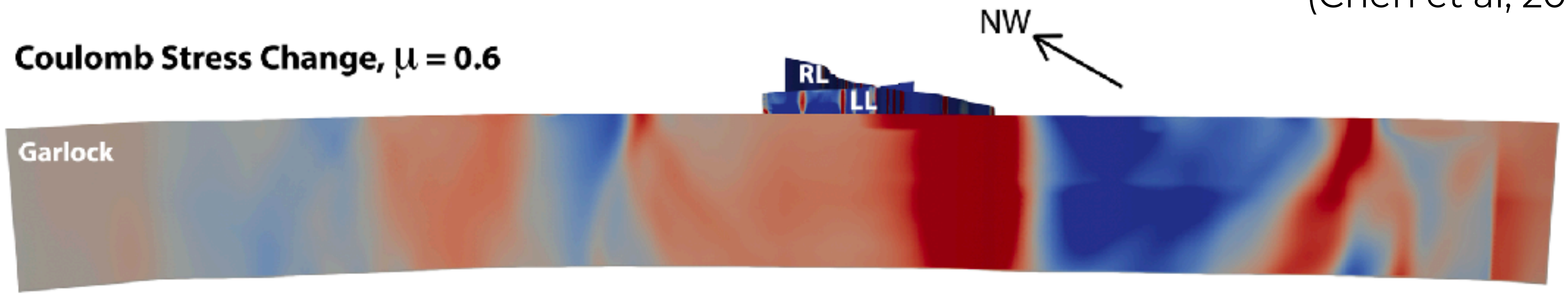

(Lozos and Harris, 2020)

Earthquake source dynamics

Well-recorded earthquakes, as the 2019 M6.4 and M7.1 Ridgecrest sequence, reveal a **striking variability in earthquake source dynamics**

- Multi-fault, hierarchical interlocked orthogonal ruptures challenging seismic hazard practices (Ross et al. 2019)

- Cascading, compound ruptures with variability of rupture styles (cracks and pulses, Chen et al. 2019)

- Dynamic and static fault interaction may have confined events and driven aftershocks/ creep on the Garlock Fault (Lozos and Harris, 2020; Barnhart et al., 2020, Ramos et al., 2020)

Gareth Funning
@gfun

Ken Hudnut (@HudnutKen): Early reconnaissance photos of the Ridgecrest earthquakes are valuable for unpicking what happened. There seems to be rupture (in the M6.4) and then re-rupture (in the M7.1) of both of the main source faults in the vicinity of their intersection. Wowsers!

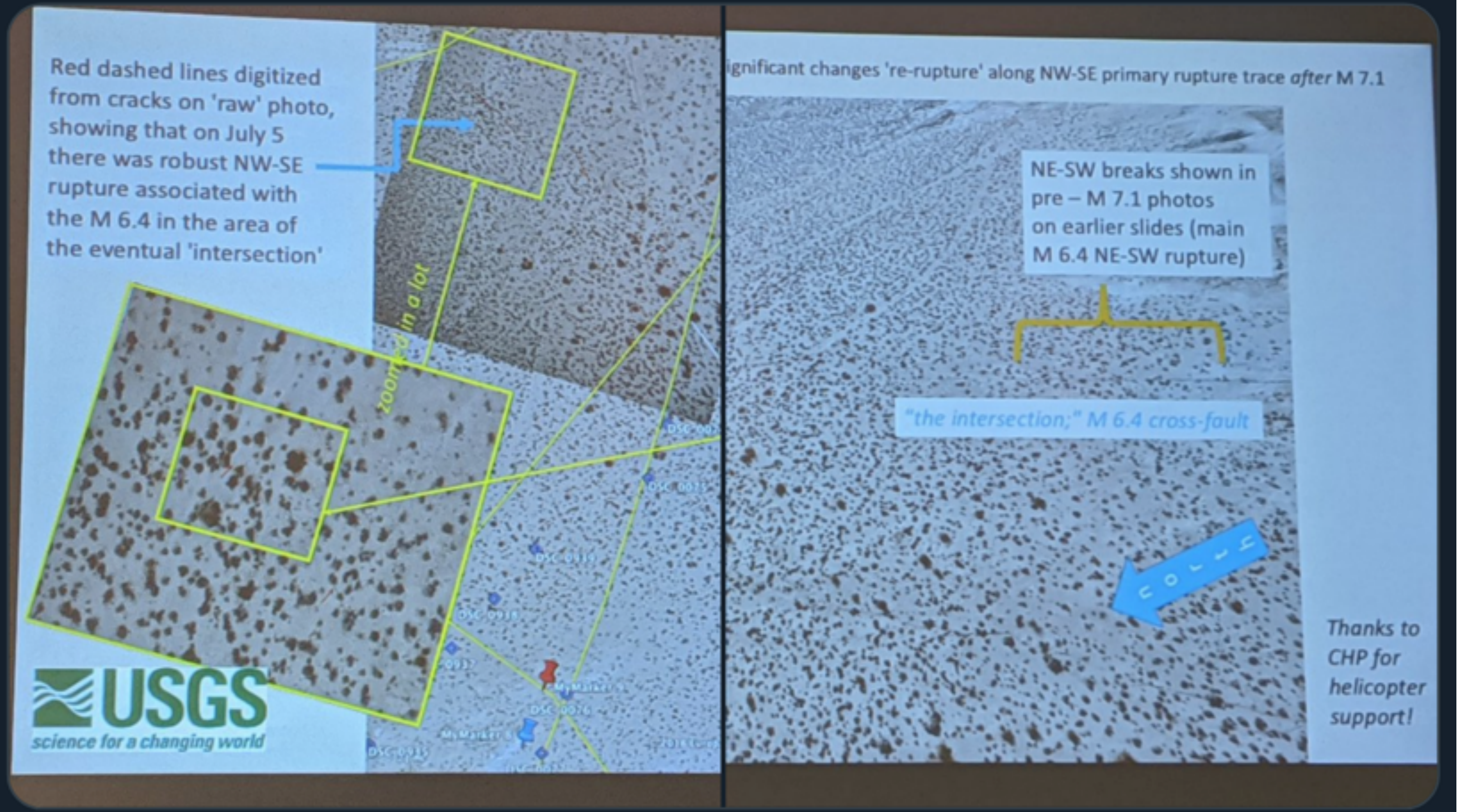

8:18 PM · Jan 28, 2020 from Menlo Park, CA · Twitter for Android

Adapted from Harris et al., SRL 2011, 2018

Earthquake dynamic rupture modeling

“Input”

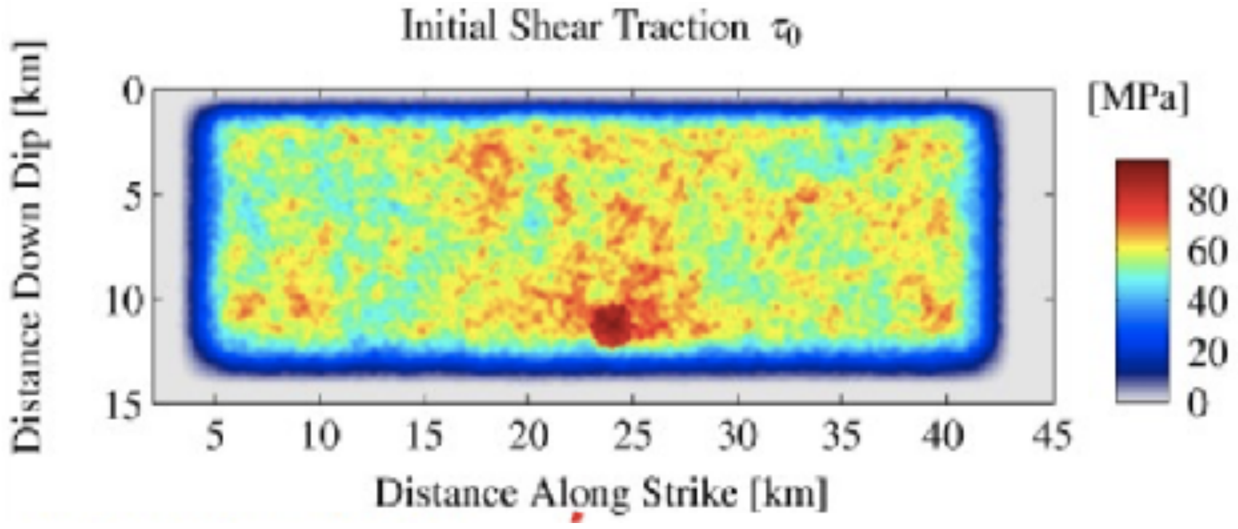

Initial fault stresses

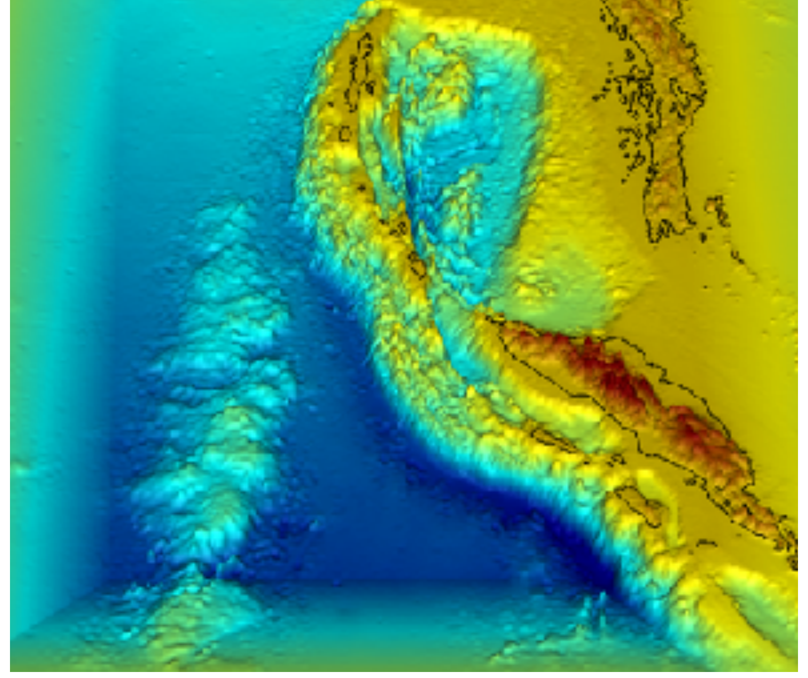

Geological structure

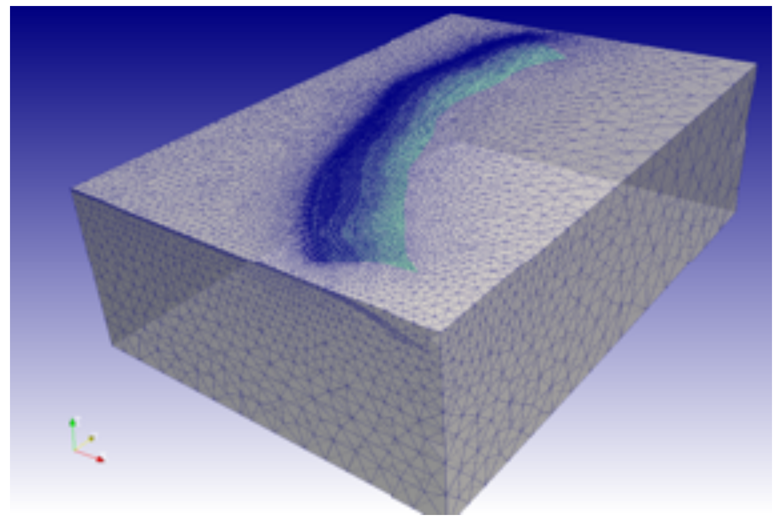

CAD & mesh generation

High-speed friction experiment (courtesy of Giulio di Toro)

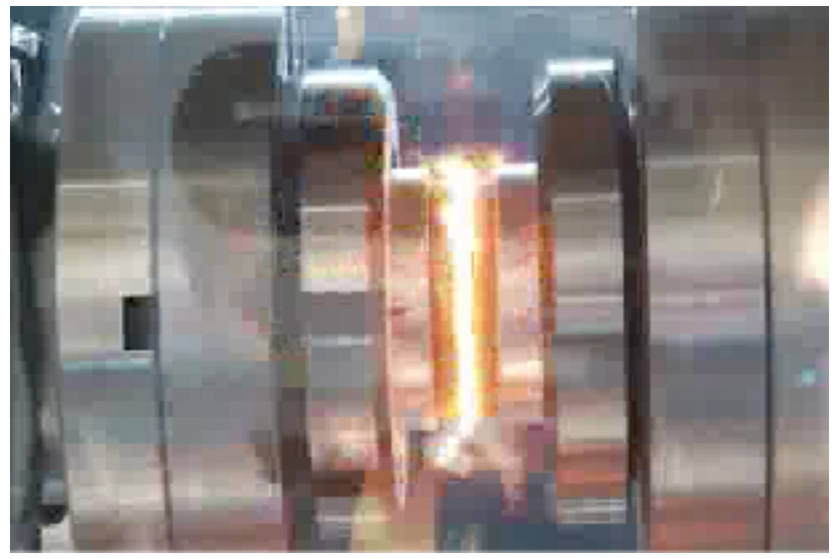

Failure Criterion

SOLVER

“Output”

Rupture dynamics

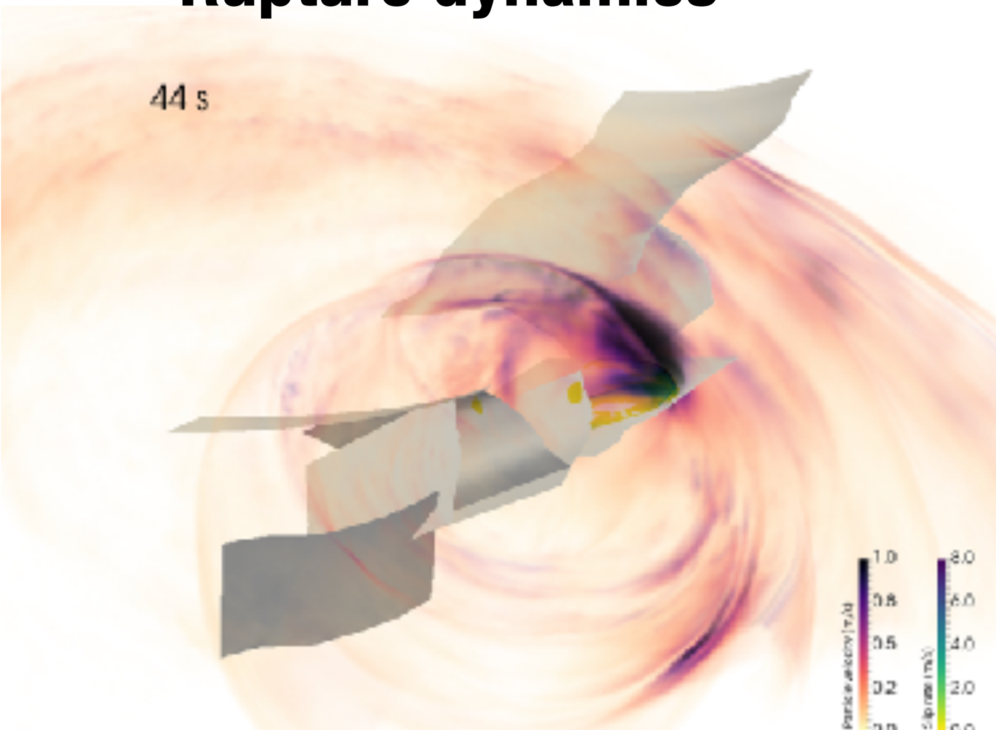

Ground deformation

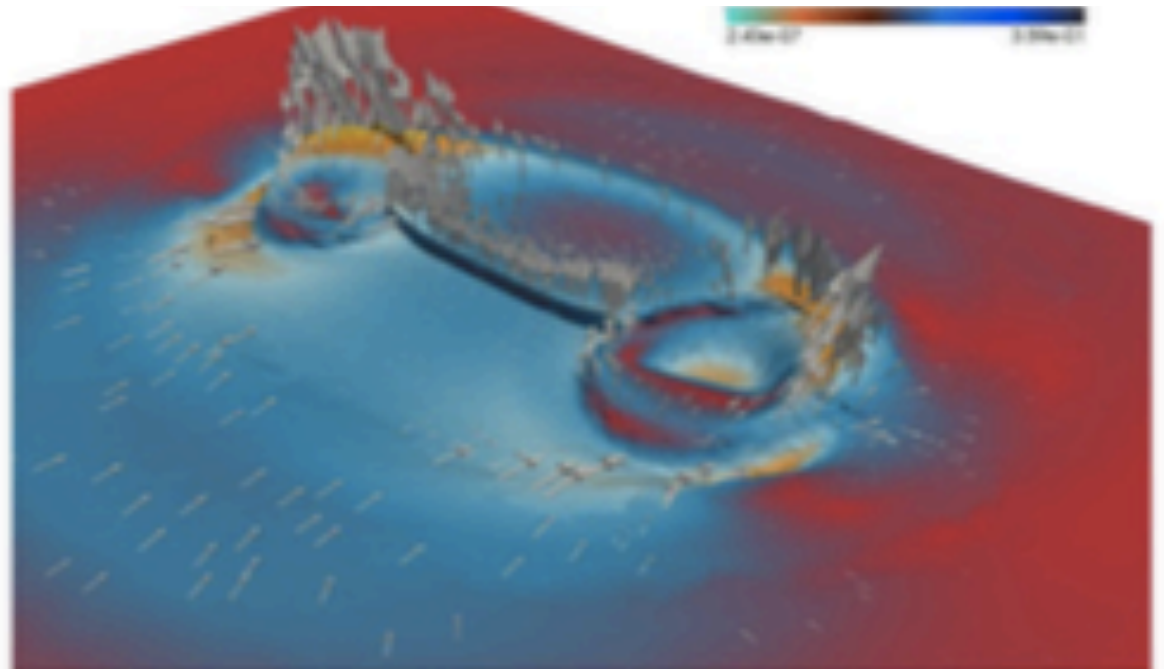

Synthetic observables

Earthquake dynamic rupture modeling

Modeling bridging scales and disciplines

- **Integrate and interpret a full range of observations** in terms of models that have meaningful fault and bulk properties from lab, field, and smaller-scale numerical studies

- **Tightly link** seismology, geodesy, geology, tectonophysics, hydrology with numerical computing, data science, machine learning, applied mathematics, continuum mechanics, tribology, rock mechanics, materials science, and engineering

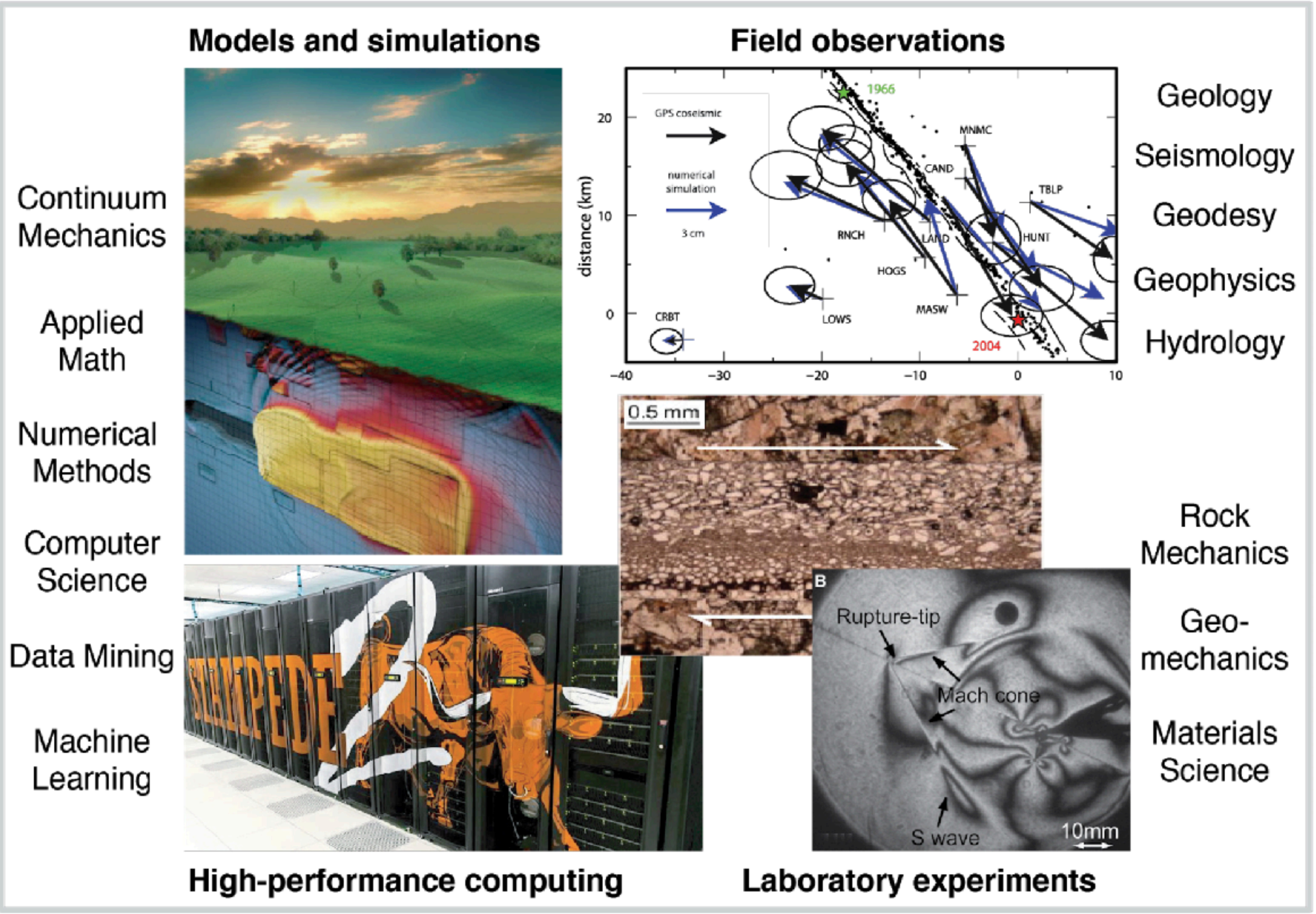

The Future of Modeling Earthquake Source Physics White Paper led by **Nadia Lapusta and Eric Dunham**, http://seismolab.caltech.edu/modeling-earthquake-source-workshop.html

Earthquake dynamic rupture modeling

Challenge 1: Earthquake source processes are (very) **ill-constrained** and **highly non-linear.**

Challenge 2: Which **physical processes** are **dominant and relevant** at a given spatio-temporal scale (and in real earthquakes)? Can we justify the "cost" of their inclusion?

Challenge 3: How to **assimilate all available knowledge** in a suitable manner for **software** (numerical discretisation, solvers, equations solved) and **hardware** (heterogeneous HPC systems, energy concerns)?

Modeling bridging scales and disciplines

- **Integrate and interpret a** … **observations** in terms of m… meaningful fault and bulk pr… field, and smaller-scale num…
- **Tightly link** seismology, ge… tectonophysics, hydrology w… computing, data science, m… applied mathematics, contin… tribology, rock mechanics, m… engineering

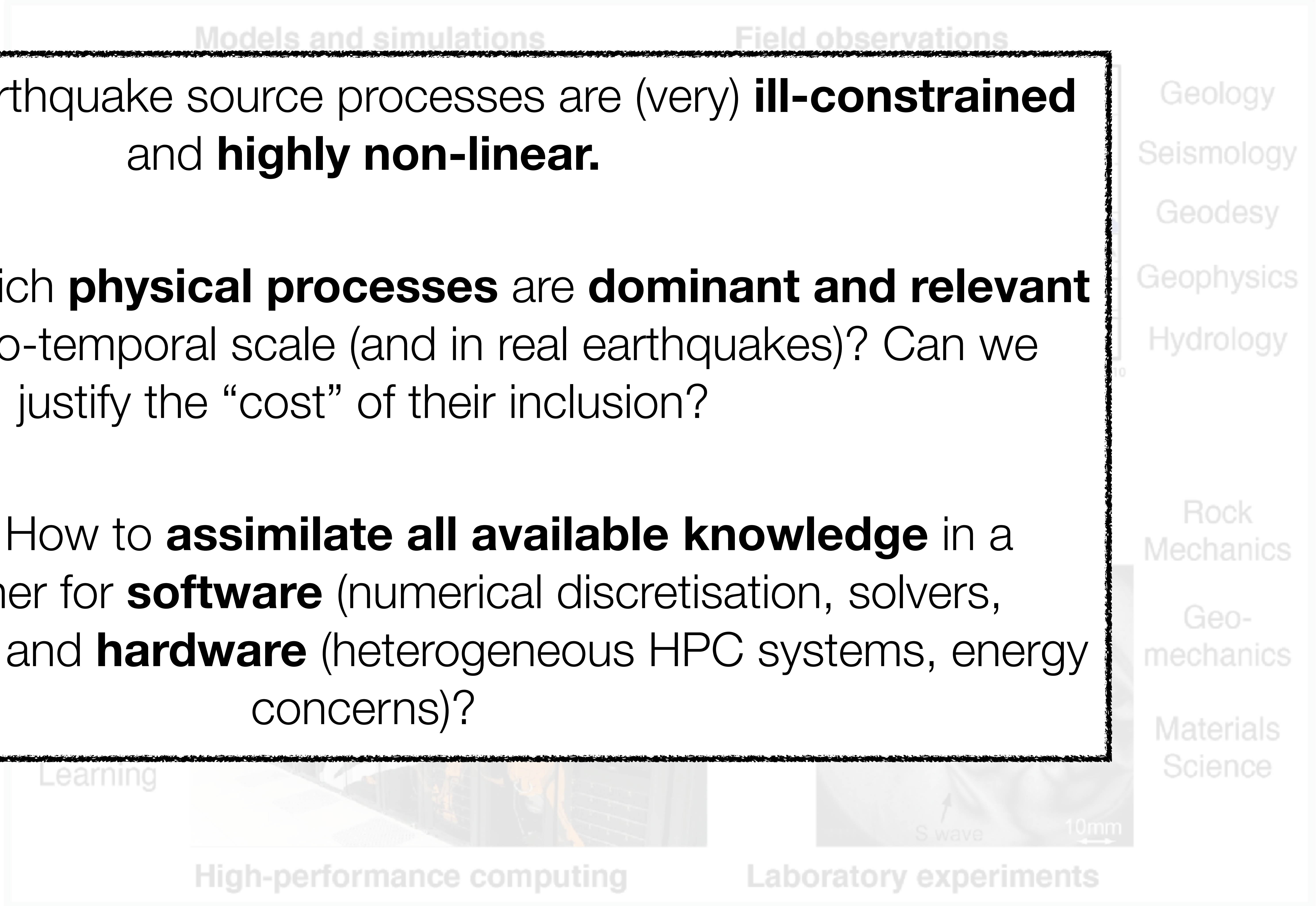

The Future of Modeling Earthquake Source Physics White Paper led by **Nadia Lapusta and Eric Dunham**, http://seismolab.caltech.edu/modeling-earthquake-source-workshop.html

Earthquake dynamic rupture modeling

Observationally constrained 3D cascading dynamic rupture scenario of the 2016, Kaikōura, NZ, earthquake (Ulrich et al., 2019, Nat. Comm.)
The Hope, Culverden and Leonard Mound faults are included but do not rupture. Multiple rupture fronts evolve, Point Kean, Papatea and Kekerengu segments slip more than once.

- **Physics-based approach:** Solving for spontaneous dynamic earthquake rupture as non-linear interaction of frictional failure and seismic wave propagation
- **Earthquake =** frictional shear failure of brittle solids under compression along preexisting weak interfaces
- **Displacement discontinuity** across the fault = **slip**
- We **"bootstrap"** on numerical methods originally not developed for earthquake source modelling (but for computational seismology)
- Much **complexity** lives in the definition of **friction** (how shear traction is bounded by fault strength), and in **fault zone complexity** as fault geometry and intersections, seismic/geodetic 'asperities', …

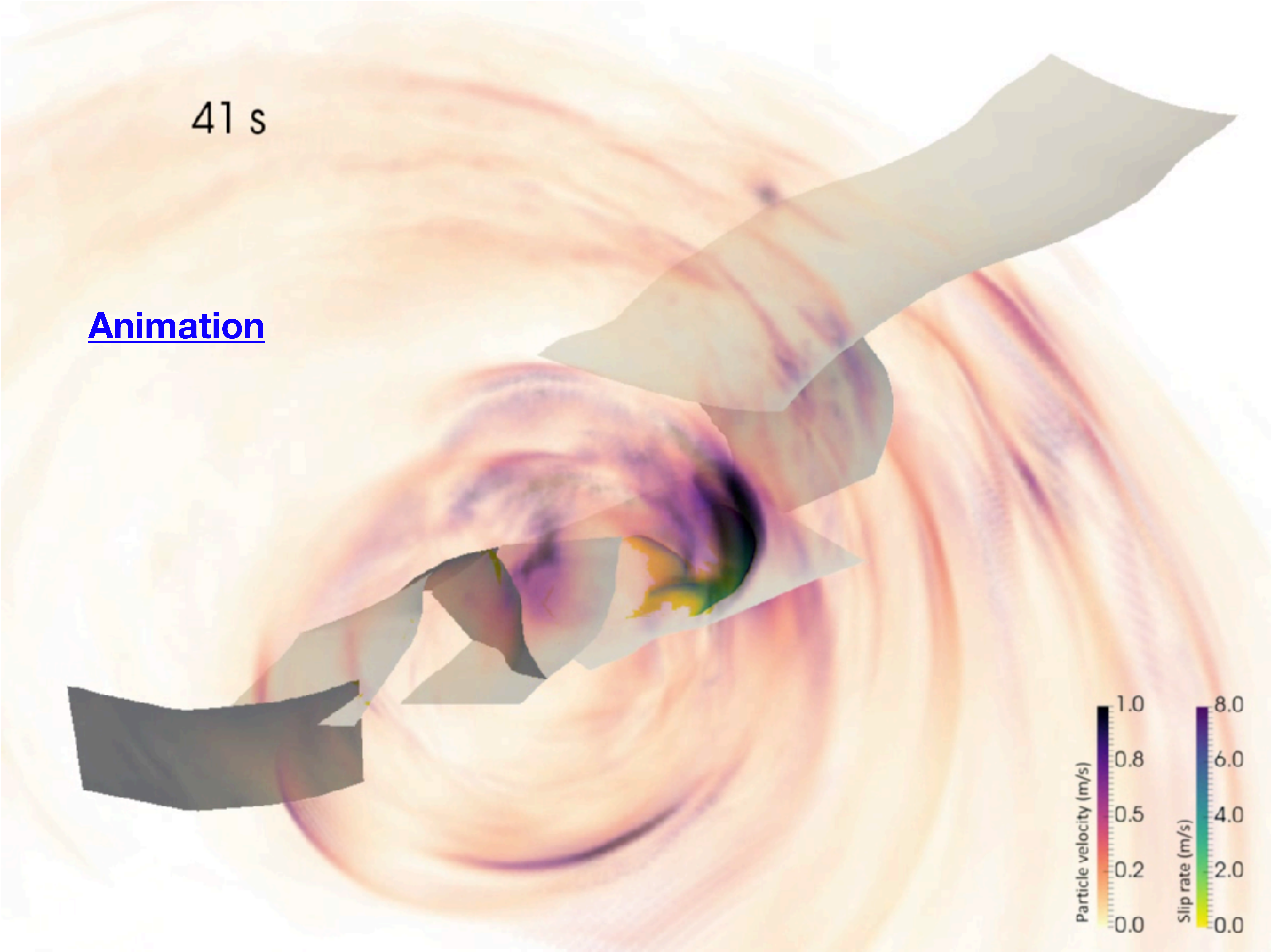

Empowered by supercomputing

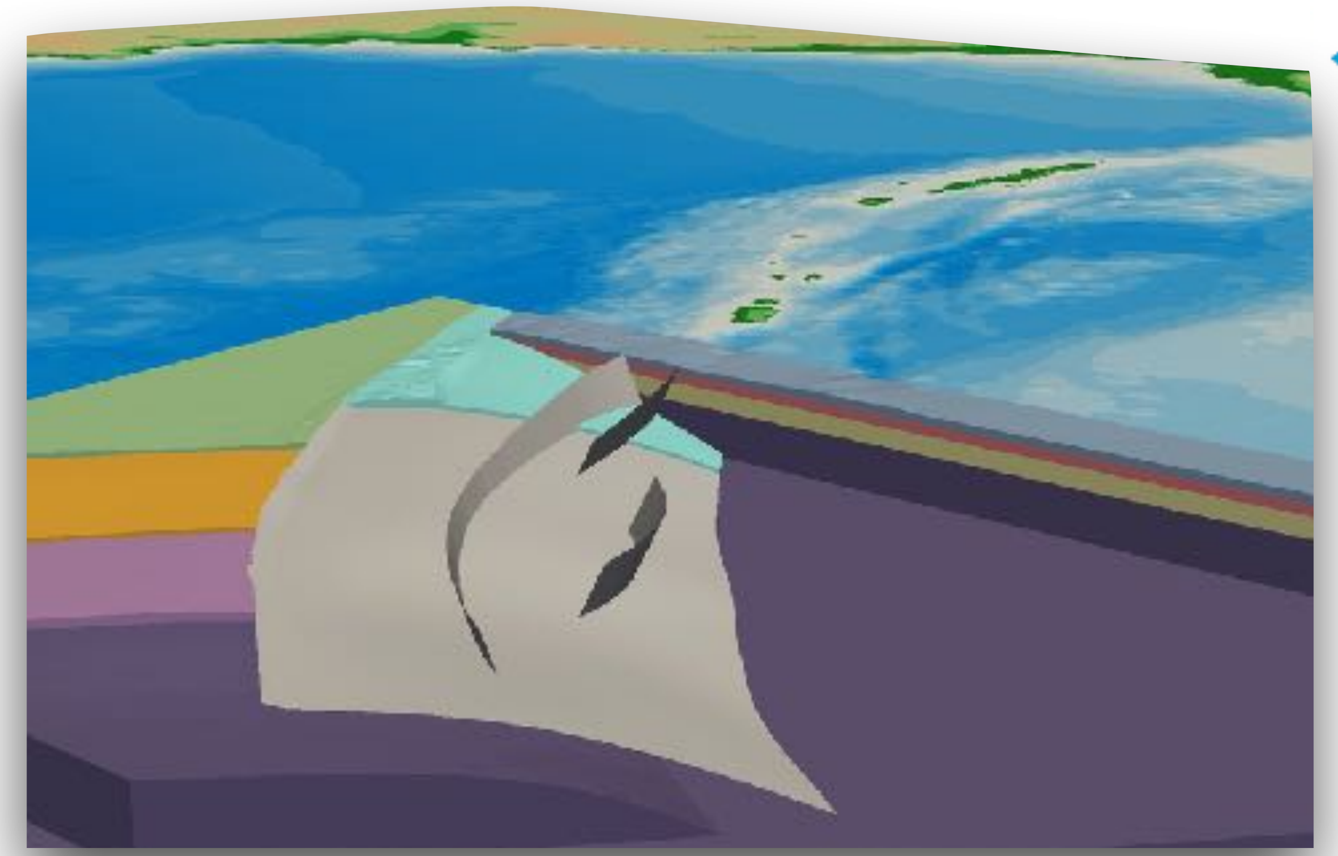

BEST PAPER

Uphoff et al., SC17

We use the open source software **SeisSol** (www.seissol.org) exploiting **unstructured tetrahedral meshes and high-order accuracy** in space and time based on an ADER-DG method handling **geometric complexity** and **highly varying element sizes**

- **"Hero runs"** use full supercomputers, e.g. 2004 Great Sumatra earthquake with spatial resolution 400m on-fault, O6 and 2.2 Hz wave propagation required mesh with 220 million finite elements (~111 x 109 degrees of freedom)
- **Recent in-house developments:** a **geoinformation server** for fast and **asynchronous input/output**, **local time stepping**, flexible boundary conditions (e.g. **gravity,** with Eric Dunham's group), towards **GPU optimisation**

Dynamic rupture and tsunami simulations of the 2004 Sumatra-Andaman event

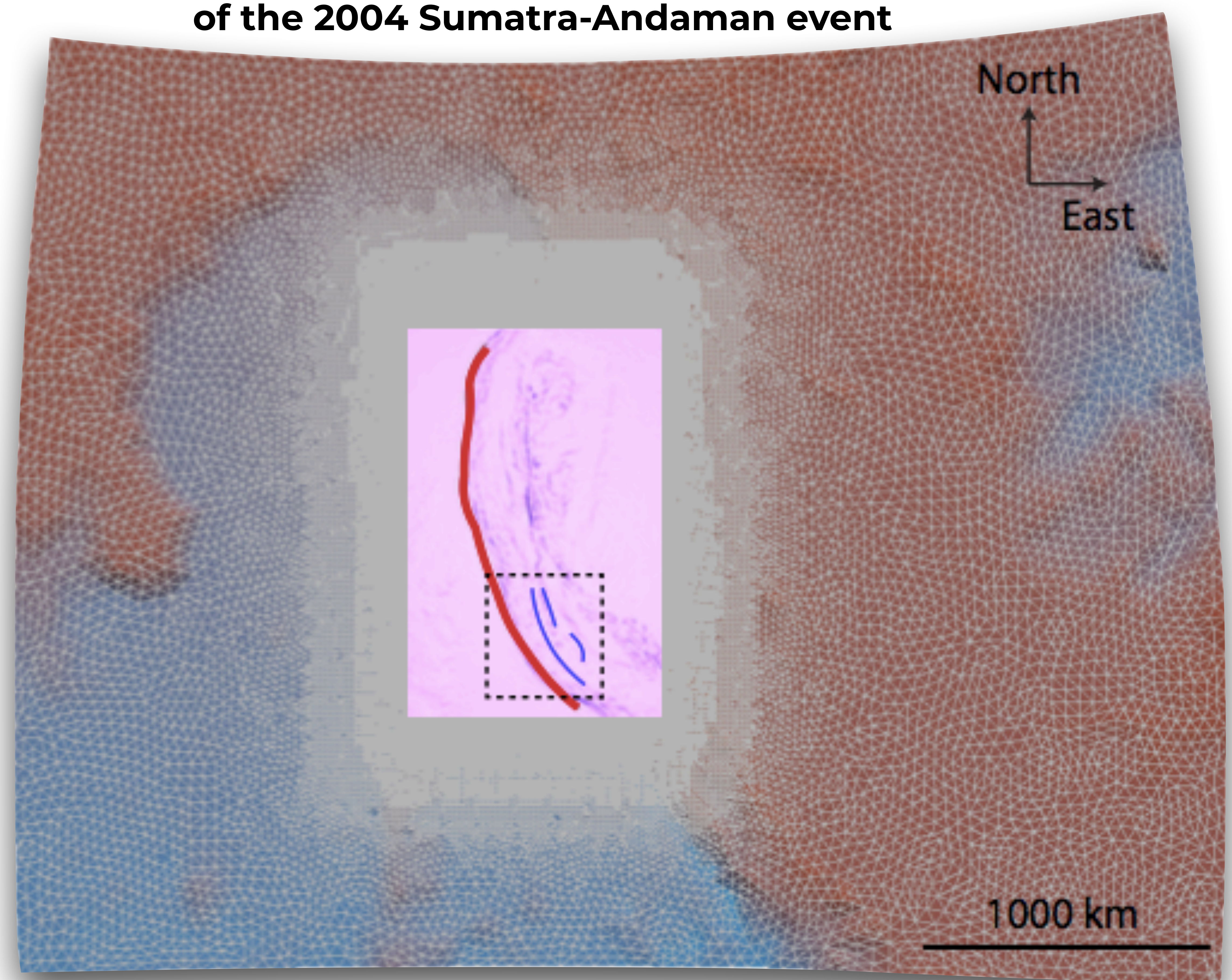

Breuer et al.,ISC14, Heinecke et al.,SC14
Breuer et al.,IEEE16, Heinecke et al.,SC16
Rettenberger et al., EASC16
Uphoff & Bader, HPCS'16

github.com/SeisSol

TECHNISCHE UNIVERSITÄT MÜNCHEN

Leibniz-Rechenzentrum der Bayerischen Akademie der Wissenschaften

Empowered by supercomputing

Breuer et al.,ISC14, Heinecke et al.,SC14
Breuer et al.,IEEE16, Heinecke et al.,SC16
Rettenberger et al., EASC16
Upphoff & Bader, HPCS'16
Uphoff et al., SC17

1992 Landers earthquake dynamic rupture scenario (10 Hz), SC14

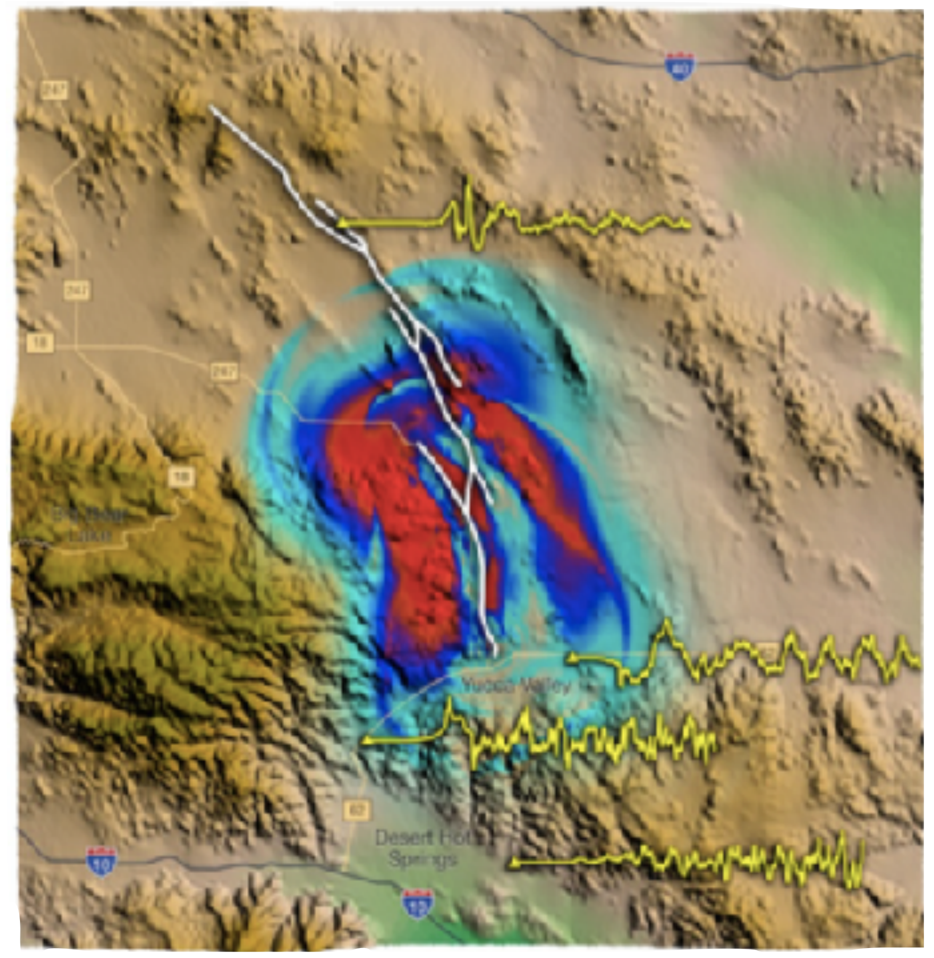

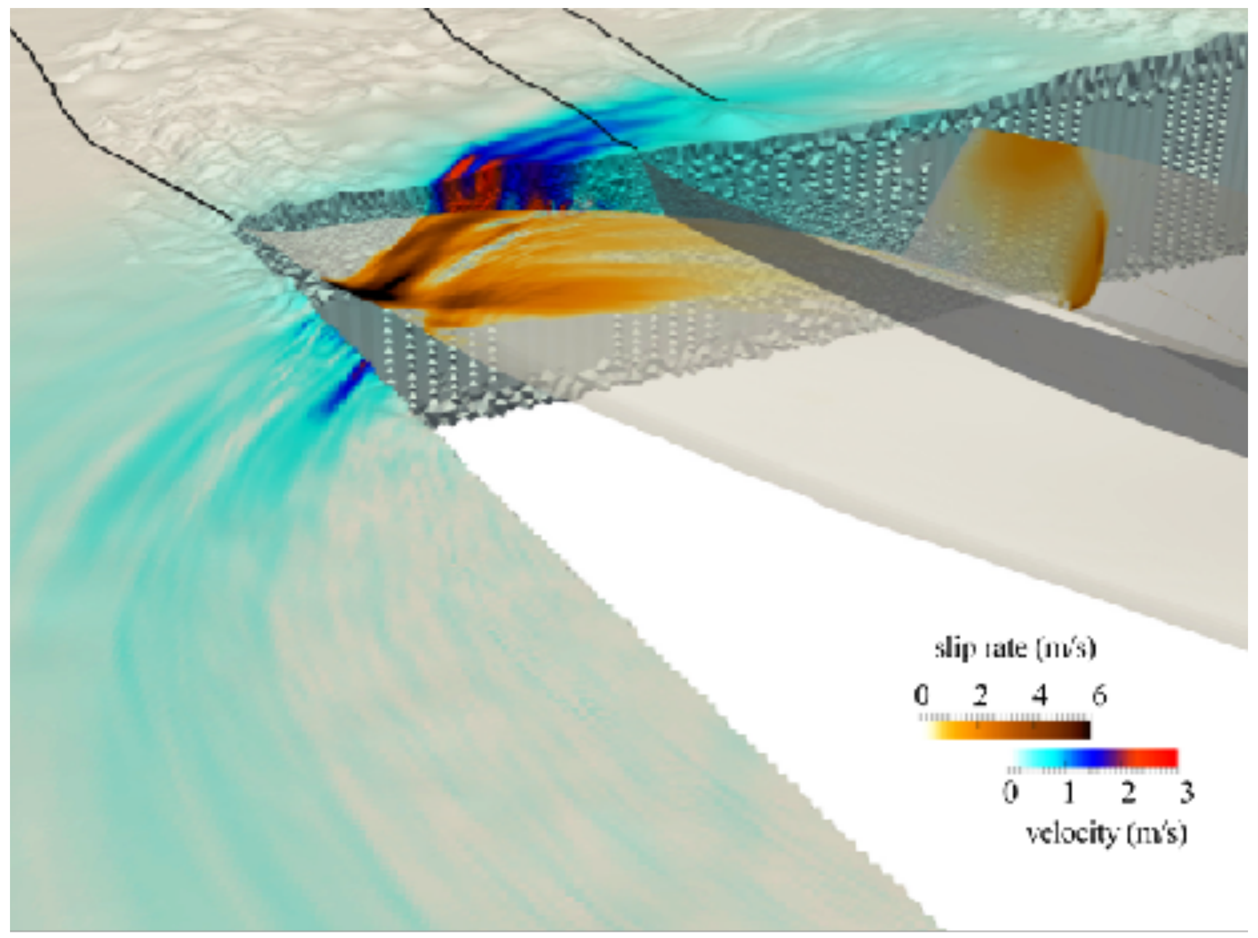

1500 km of faults, 2.5 Hz wavefield, linked to tsunami simulations, SC17

"Geophysics" Version

- Fortran 90
- MPI parallelised
- Ascii based, serial I/O

AWARDS Gordon Bell Prize

Landers scenario
(96 billion DoF, 200,000 time steps)

- Hybrid MPI+OpenMP parallelisation
- Parallel I/O (HDF5, inc. mesh init.)
- Assembler-level DG kernels
- multi-physics off-load scheme for many-core architectures

- > 1 PFlop/s performance
- 90% parallel efficiency
- 45% of peak performance
- 5x-10x faster time-to-solution
- 10x-100x bigger problems

SC17 BEST PAPER

Sumatra scenario
(111 billion DoF, 3,300,000 time steps)

- Cluster-based local time stepping
- Code generator also for advanced PDE's as viscoelastic attunation
- Asagi (XDMF)-geoinformation server
- Asynchronous input/output
- Overlaping computation and communication

- Optimized for Intel KNL
- Speed up of 14x
- 14 hours compared to almost 8 days for Sumatra scenario on SuperMuc2

Open-source software that allows for rapid setup of models with realistic non-planar and intersecting fault systems while exploiting the accuracy of a high-order numerical method

Dynamic rupture modeling of the 2019 Ridgecrest sequence
1. A geometrically complex 3D fault network

- We construct a **non-vertical quasi-orthogonal crosscutting 3D fault geometry** intersecting with **topography** and embedded in the **CVMS** subsurface model from integrating geological field mapping of rupture traces, geodetical InSAR data, relocated seismicity of Ross et al., 2019 and selected focal mechanisms from SCEDC catalog (Carena and Suppe, 2002)

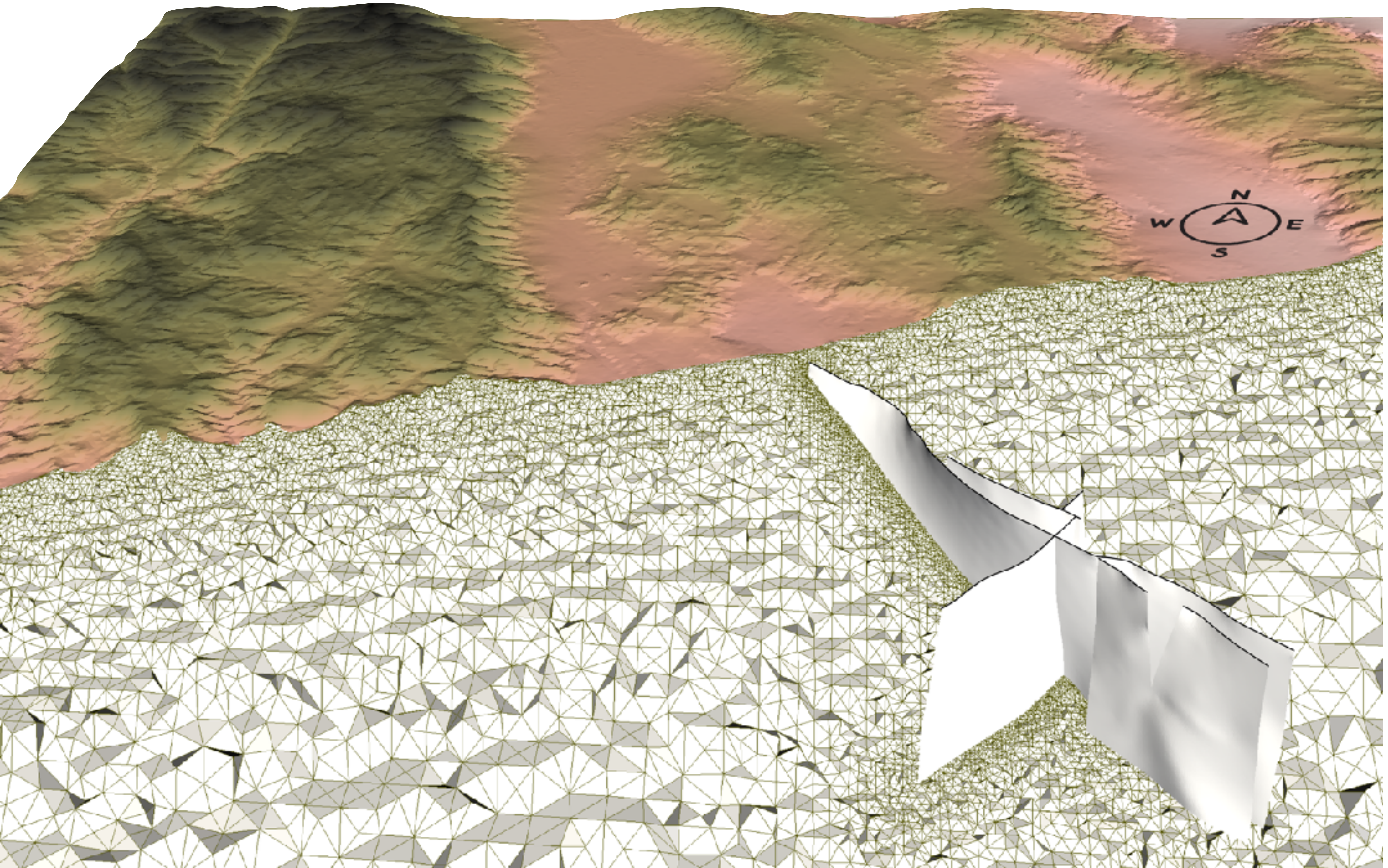

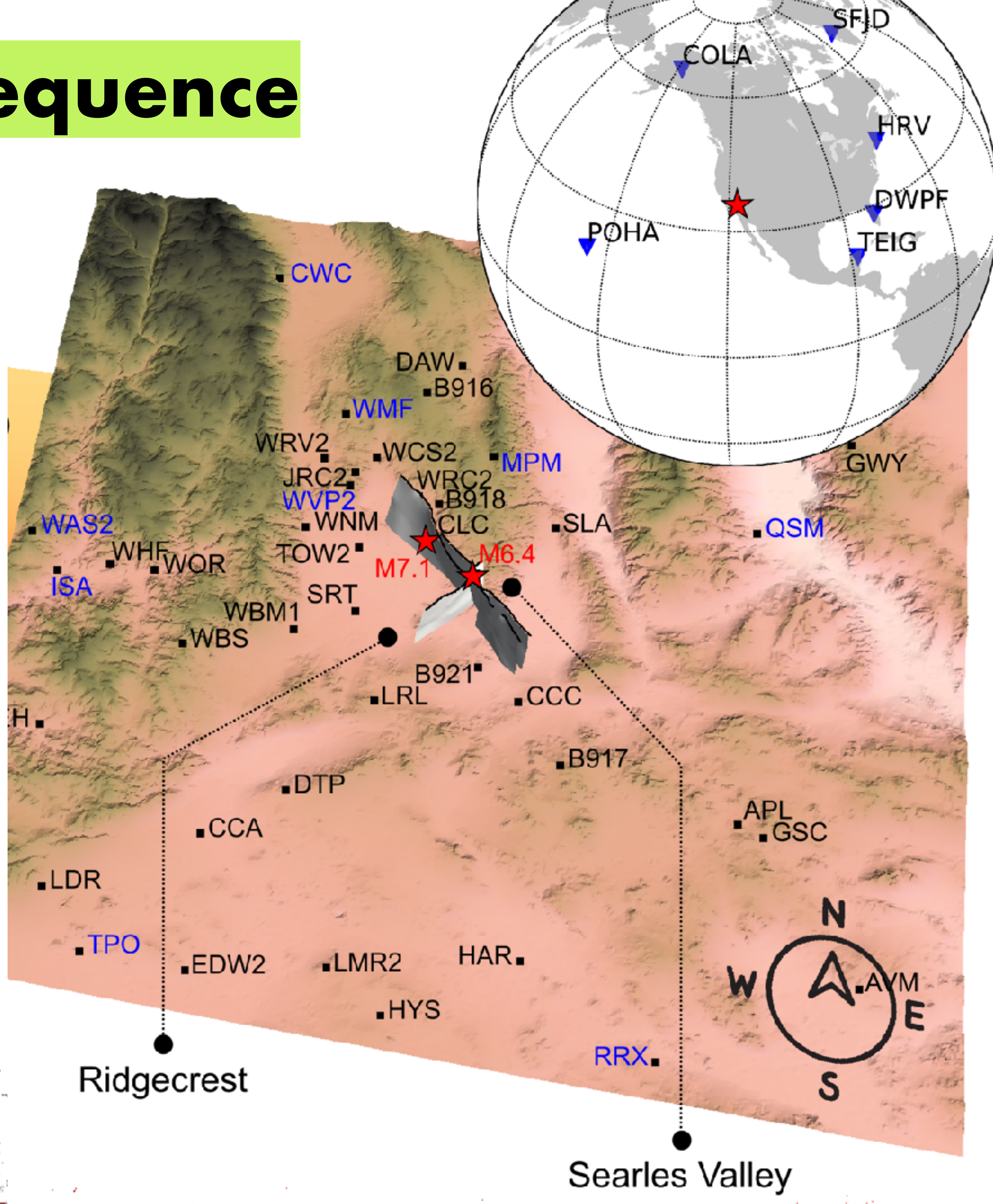

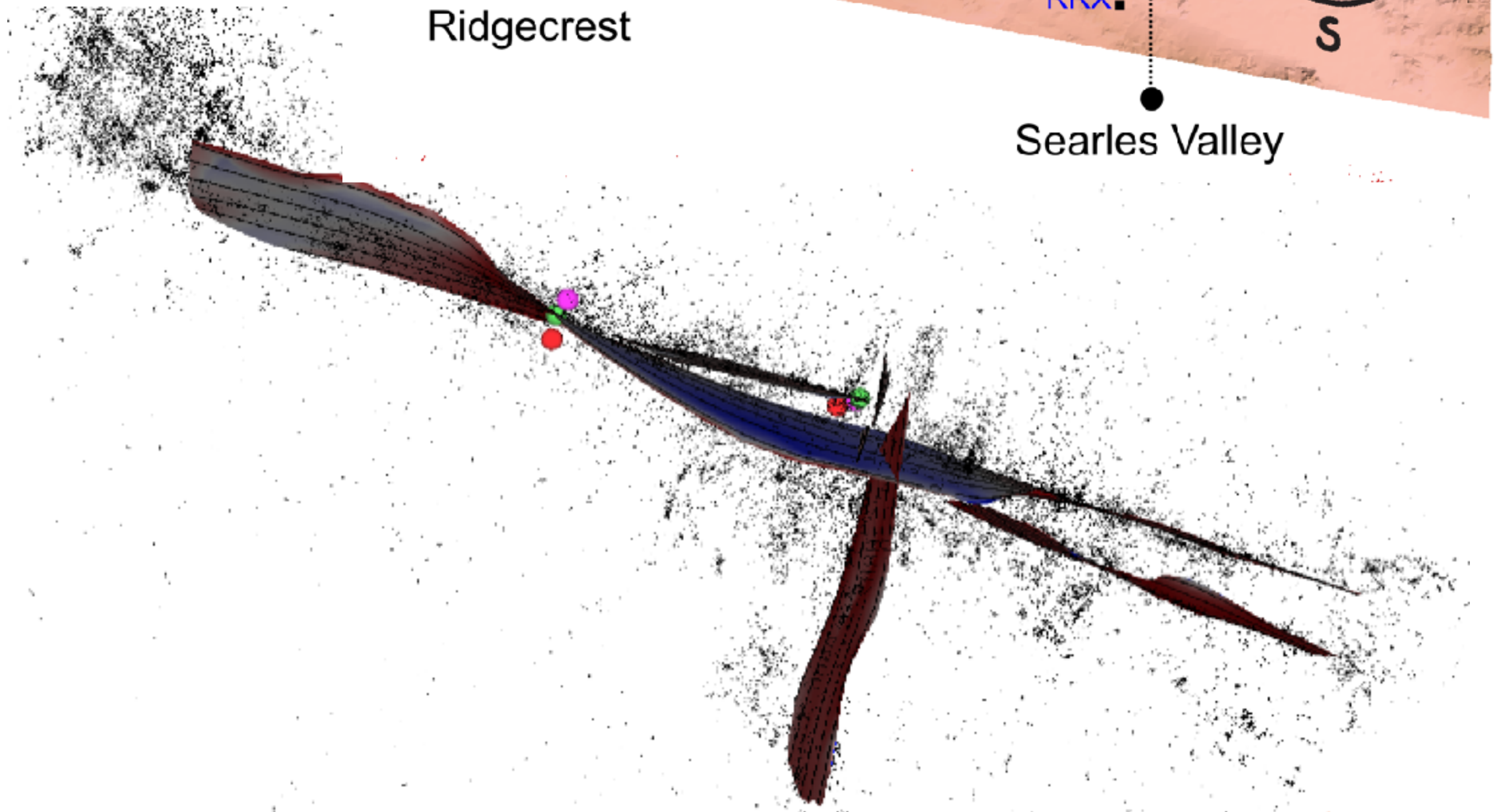

Dynamic rupture modeling of the 2019 Ridgecrest sequence
2. Initial stresses

- The dynamics of both events show a high sensitivity, specifically in the vicinity of complexities in fault geometry, **to the 3D stress state** consisting of the background loading plus long- and short-term static and dynamic stress transfers

- All faults are exposed to **3D tectonic stress state** (YHSM-2013)

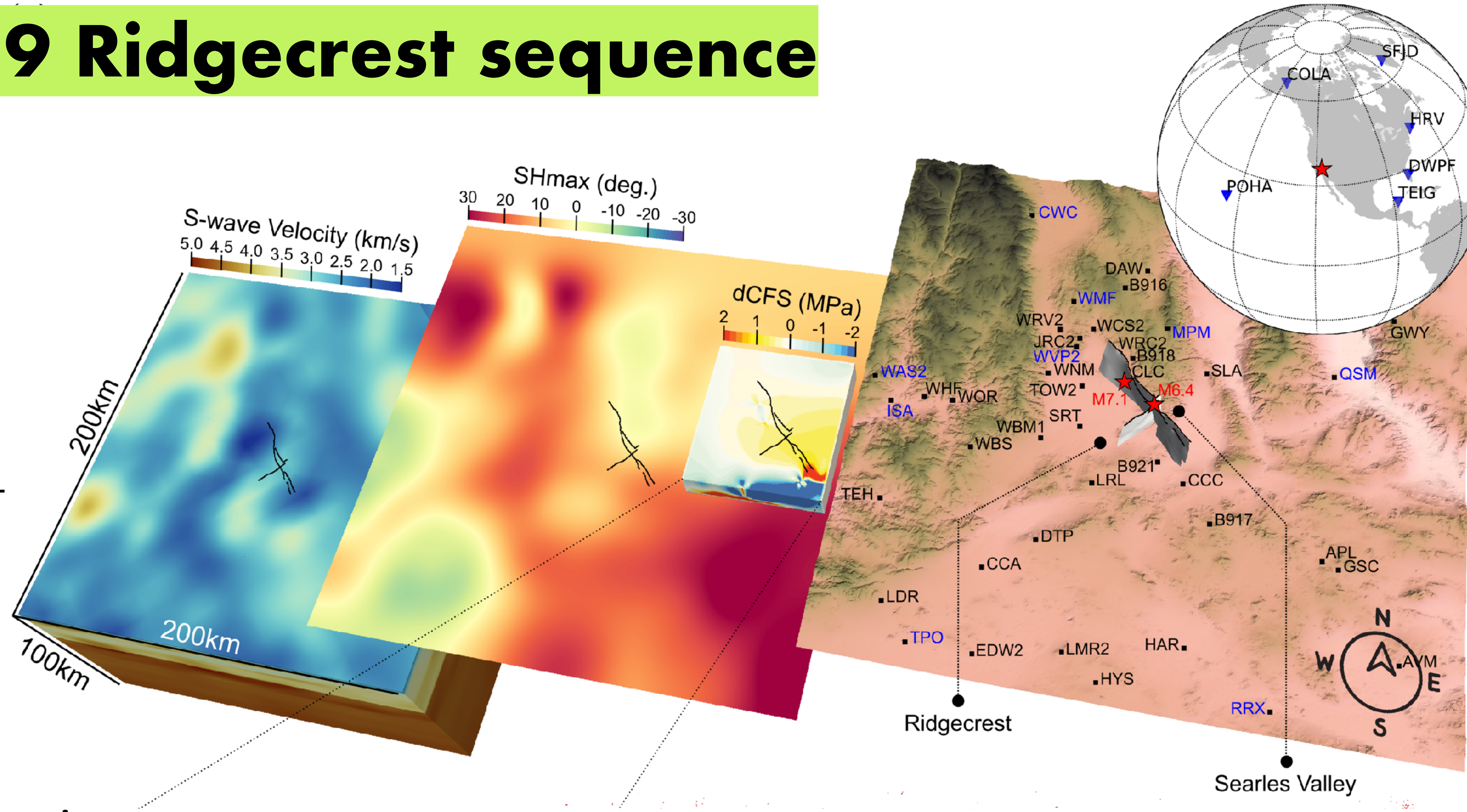

Stress-shape ratio

$$\nu = (s_2 - s_3)/(s_1 - s_3)$$

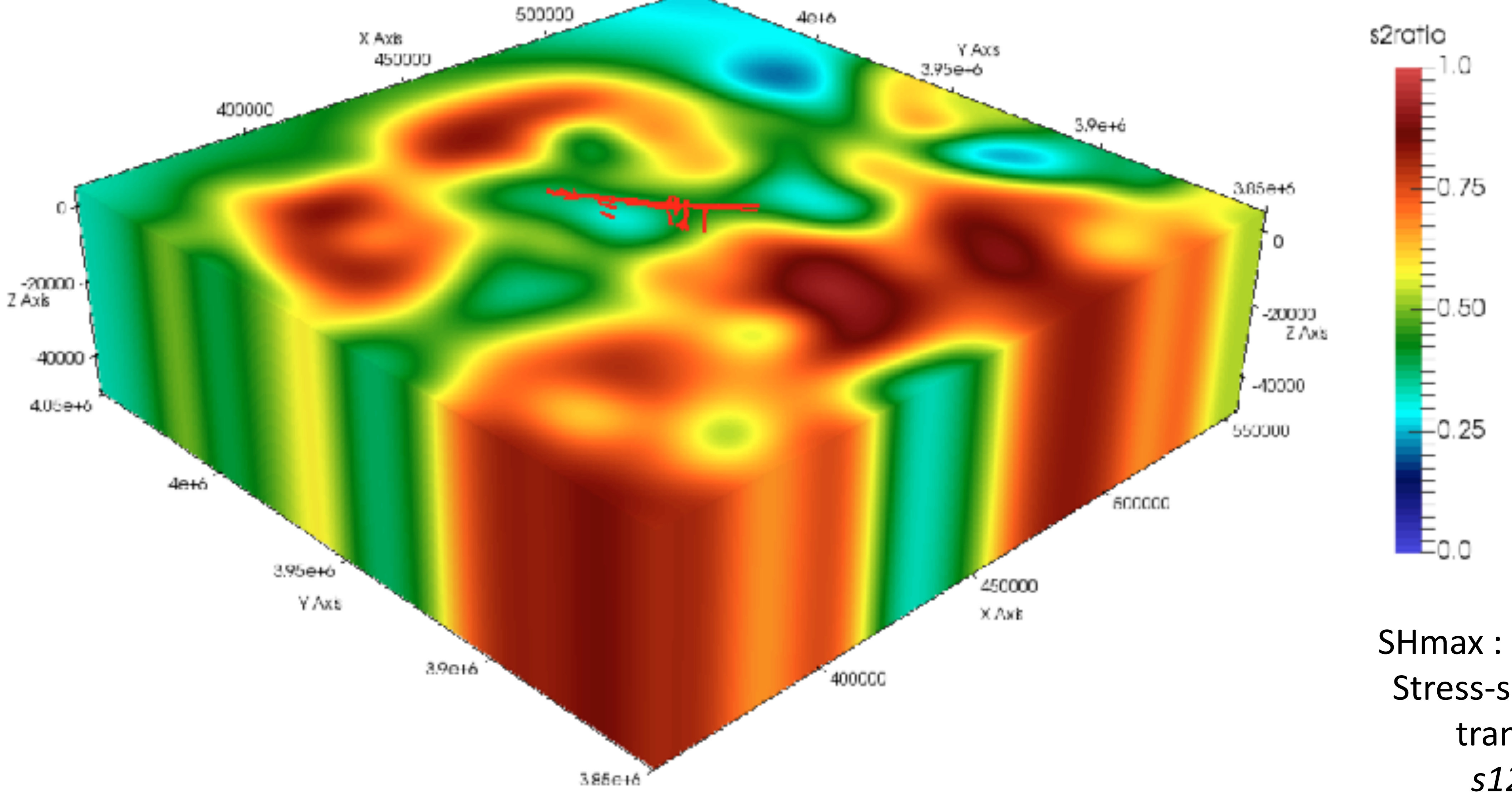

SHmax

3D SCEC Community Stress Model (CSM)
YHSM-2013, Yang & Hauksson, 2012

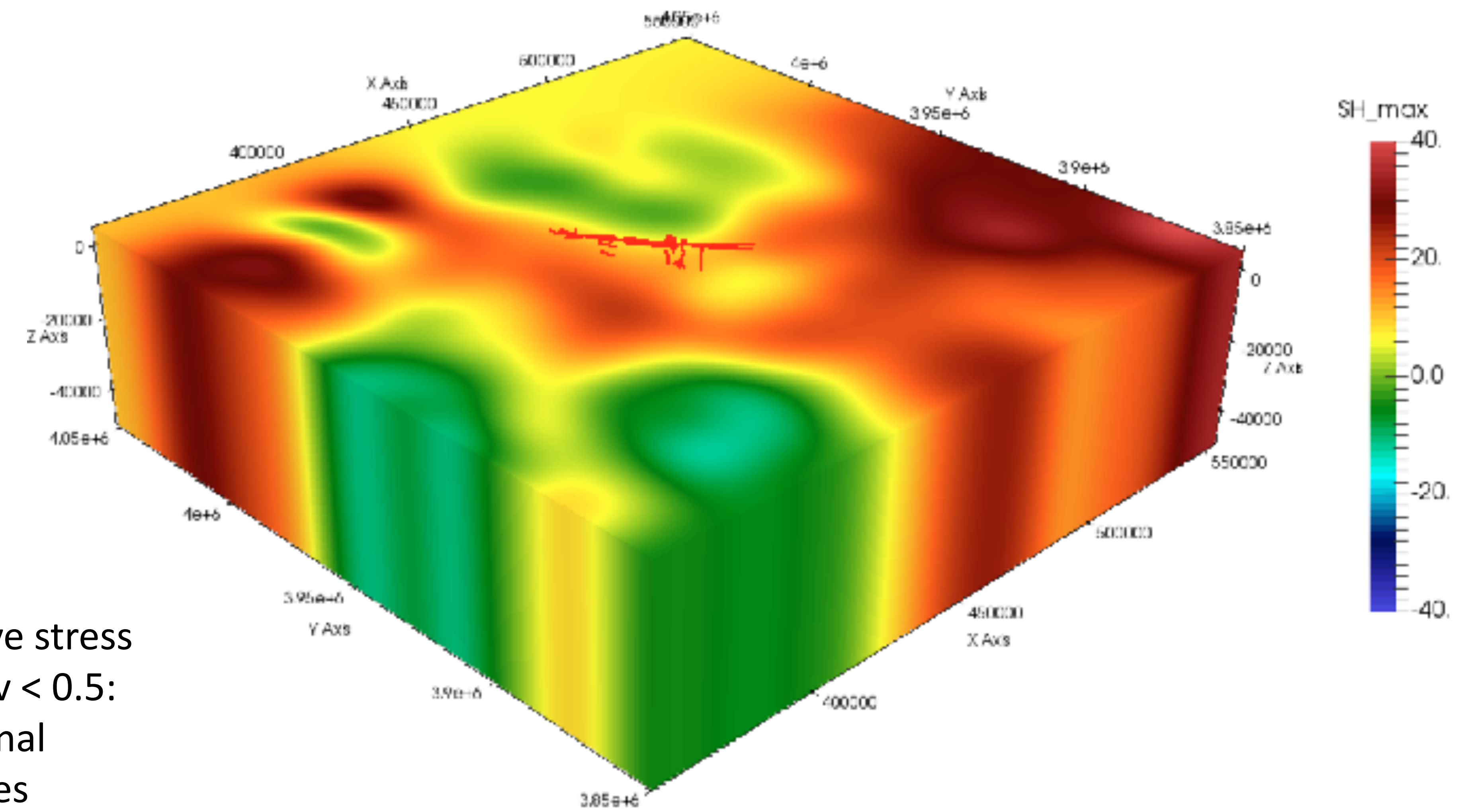

SHmax : maximum horizontal compressive stress
Stress-shape ratio (v) : style of faulting, v < 0.5: transpressional, v > 0.5: transtensional
s123: amplitude of principal stresses

Dynamic rupture modeling of the 2019 Ridgecrest sequence
2. Initial stresses

- pre-Ridgecrest **co-seismic and post-seismic Coulomb failure stress changes** (dCFS) due to previous major earthquakes occurring in the region in the last **~1400 years** (Verdecchia & Carena, 2016; Friedrich et al., 2019) yields positive stress redistribution additionally loading the source region

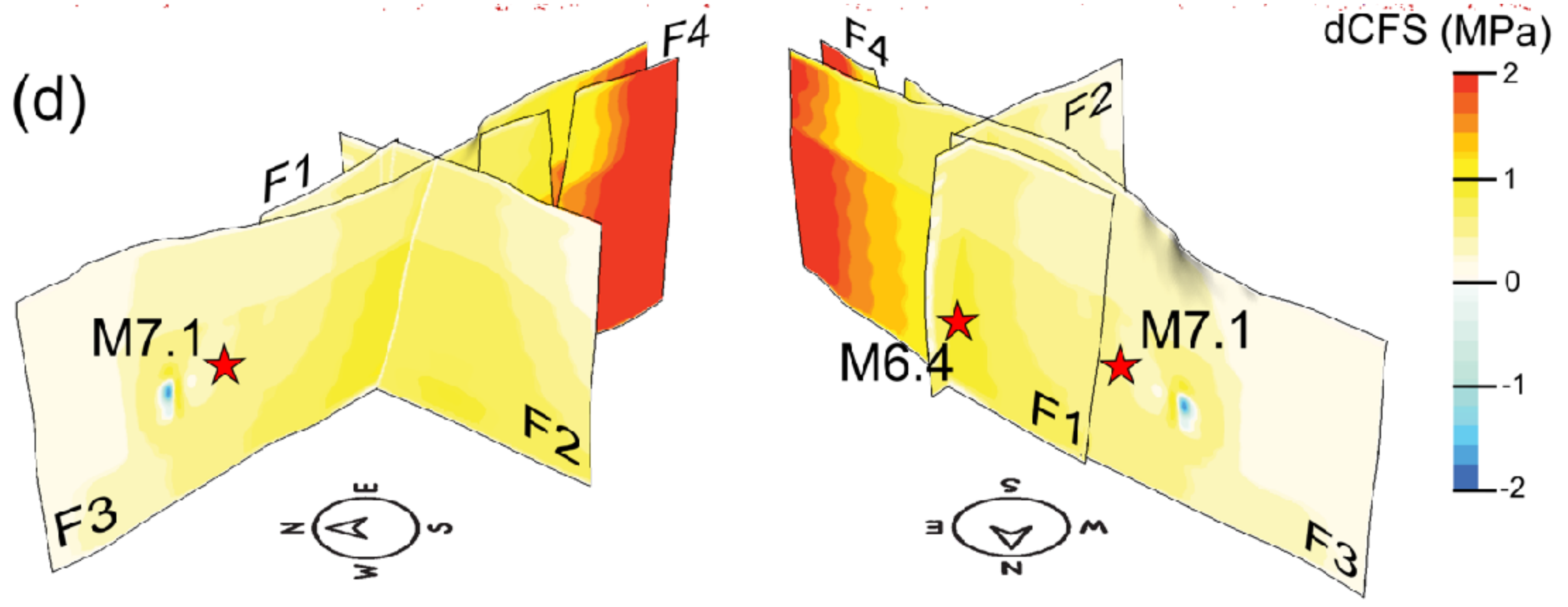

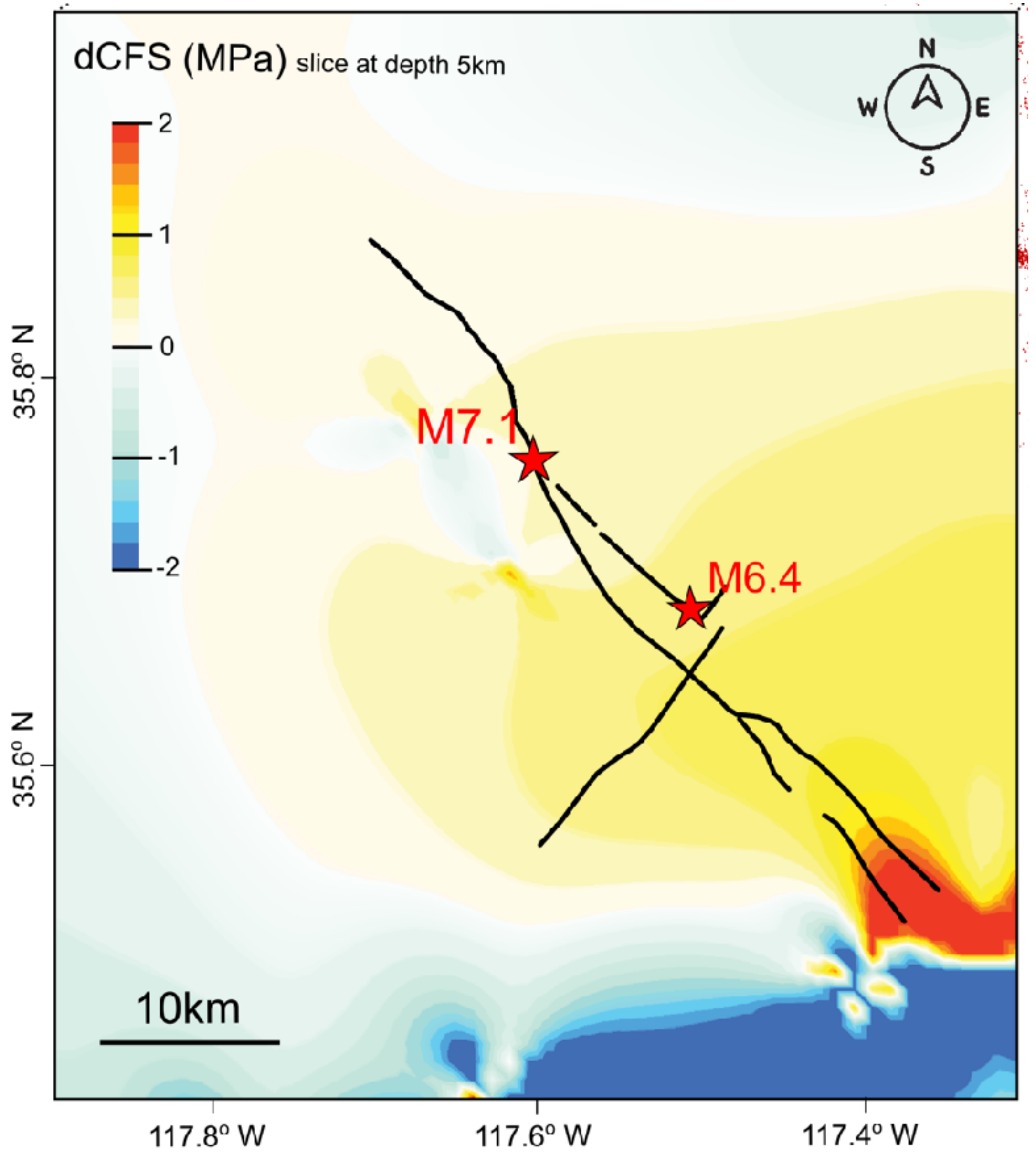

Dynamic rupture modeling of the 2019 Ridgecrest sequence
2. Initial stresses

- pre-Ridgecrest **co-seismic and post-seismic Coulomb failure stress changes** (dCFS) due to previous major earthquakes occurring in the region in the last **~1400 years** (Verdecchia & Carena, 2016; Friedrich et al., 2019) yields positive stress redistribution additionally loading the source region

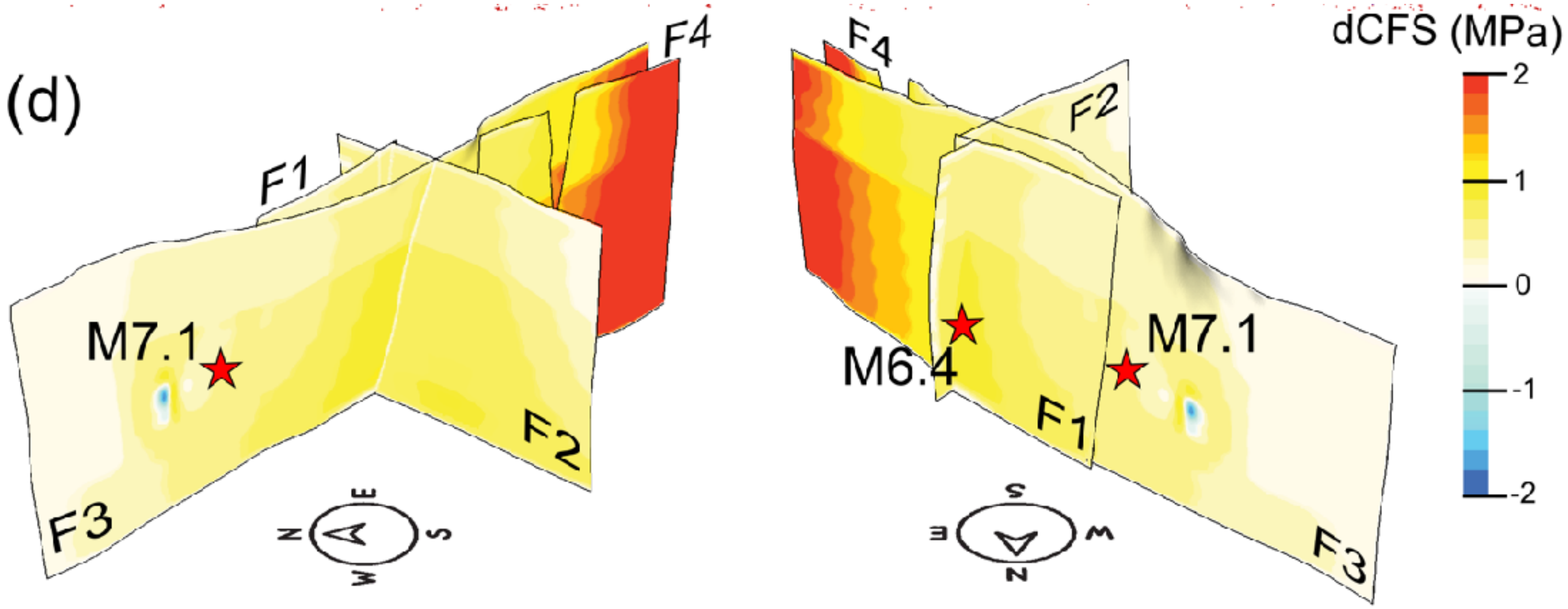

- Two **coupled dynamic rupture models** (either one continuous simulation, or using checkpointing utilities) incorporating off-fault plasticity and co-seismic dynamic/static stress transfers

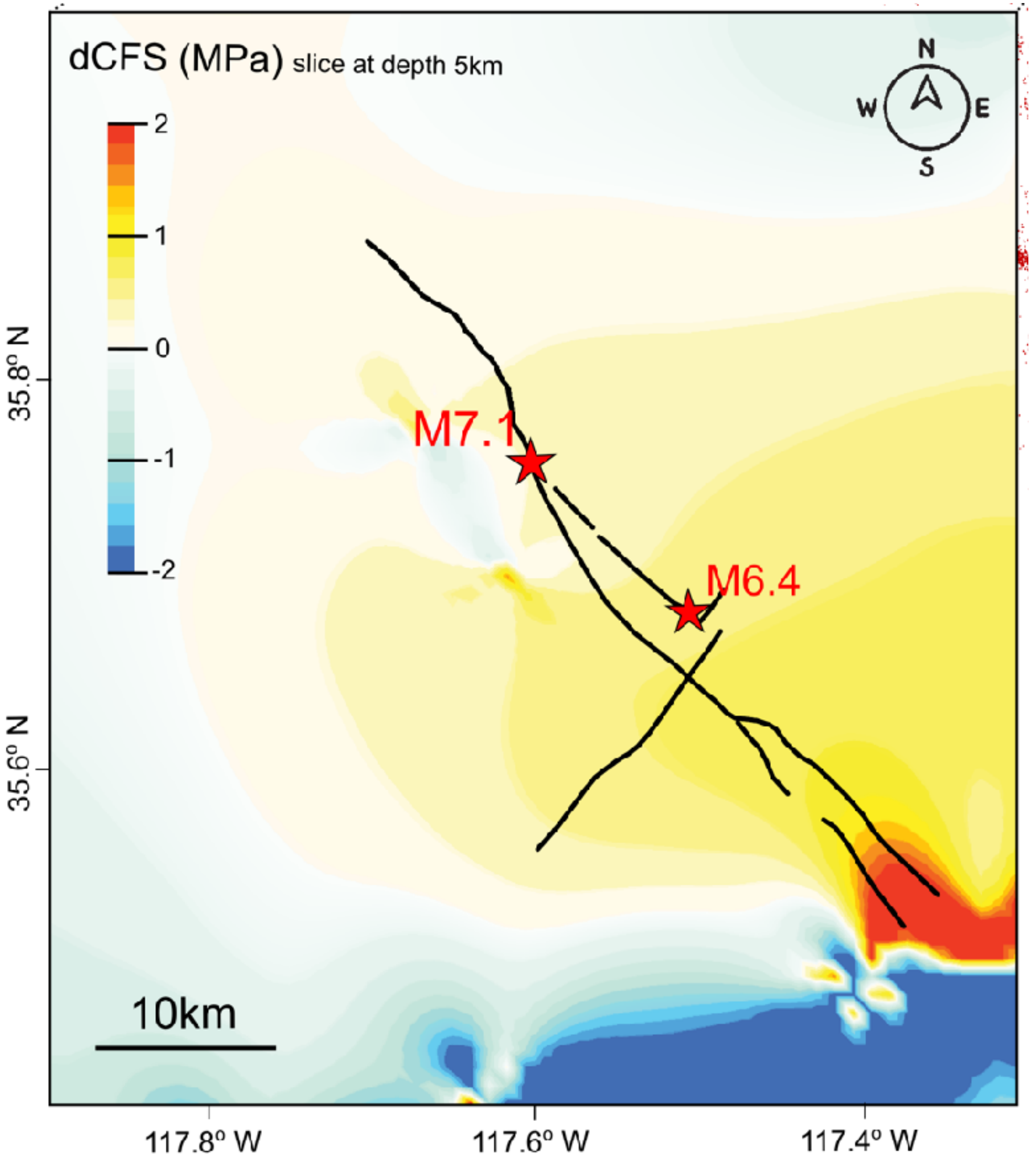

Dynamic rupture modeling of the 2019 Ridgecrest sequence
3. Fault strength

Wei et al., 2013, based on creepmeters and theodolite measurements along SAF

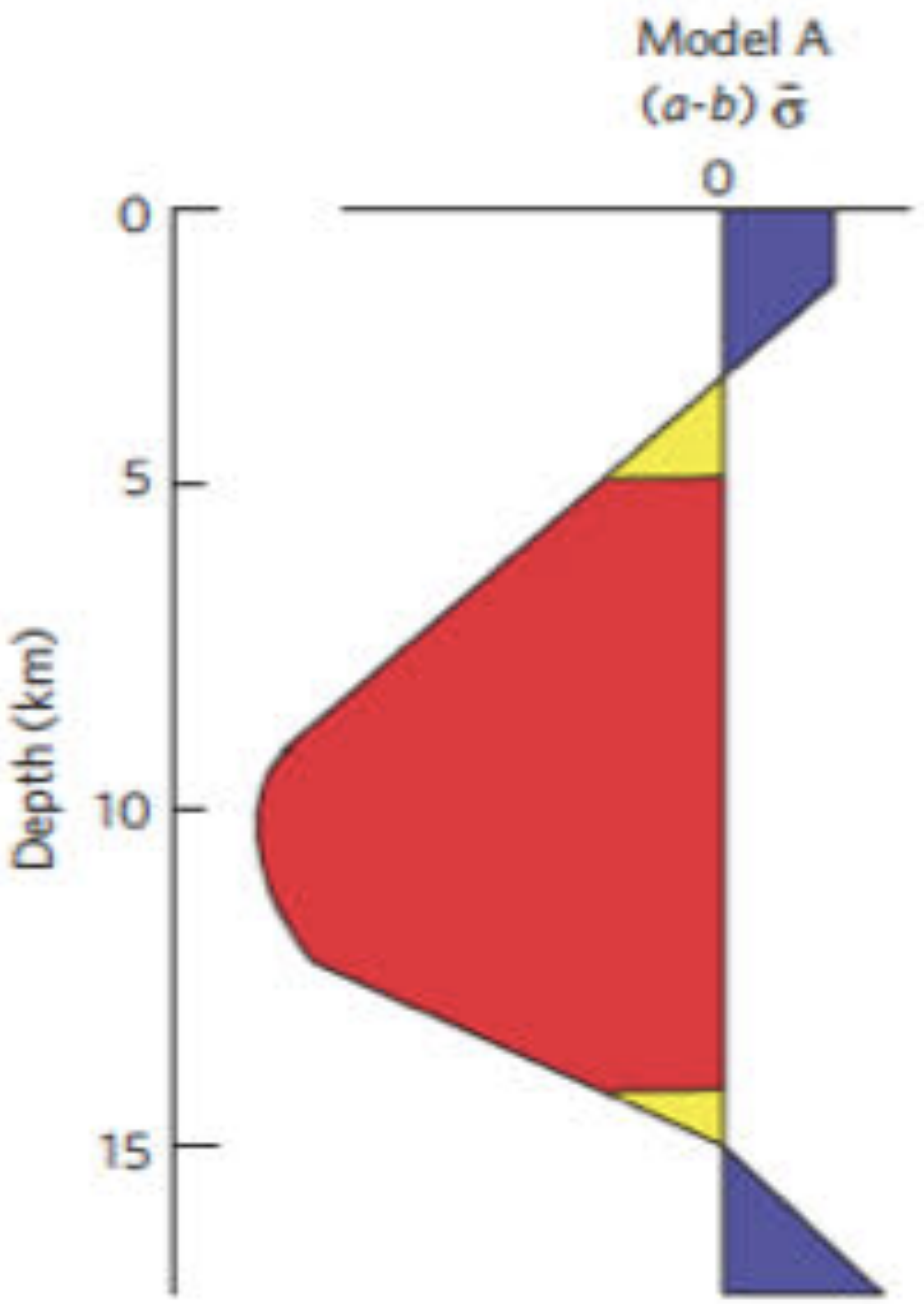

- **Apparently weak faults** due to combined effects of **severe velocity-weakening friction, elevated fluid pressure** and **fault geometry**

- Fault friction: **rate-and-state friction with rapid velocity weakening** (Dunham et al., 2011) but statically 'strong' (0.6)

Note: seismogenic depth is here adapted by seismicity (Ross et al.2019)

Dynamic rupture modeling of the 2019 Ridgecrest sequence
3. Fault strength

Wei et al., 2013, based on creepmeters and theodolite measurements along SAF

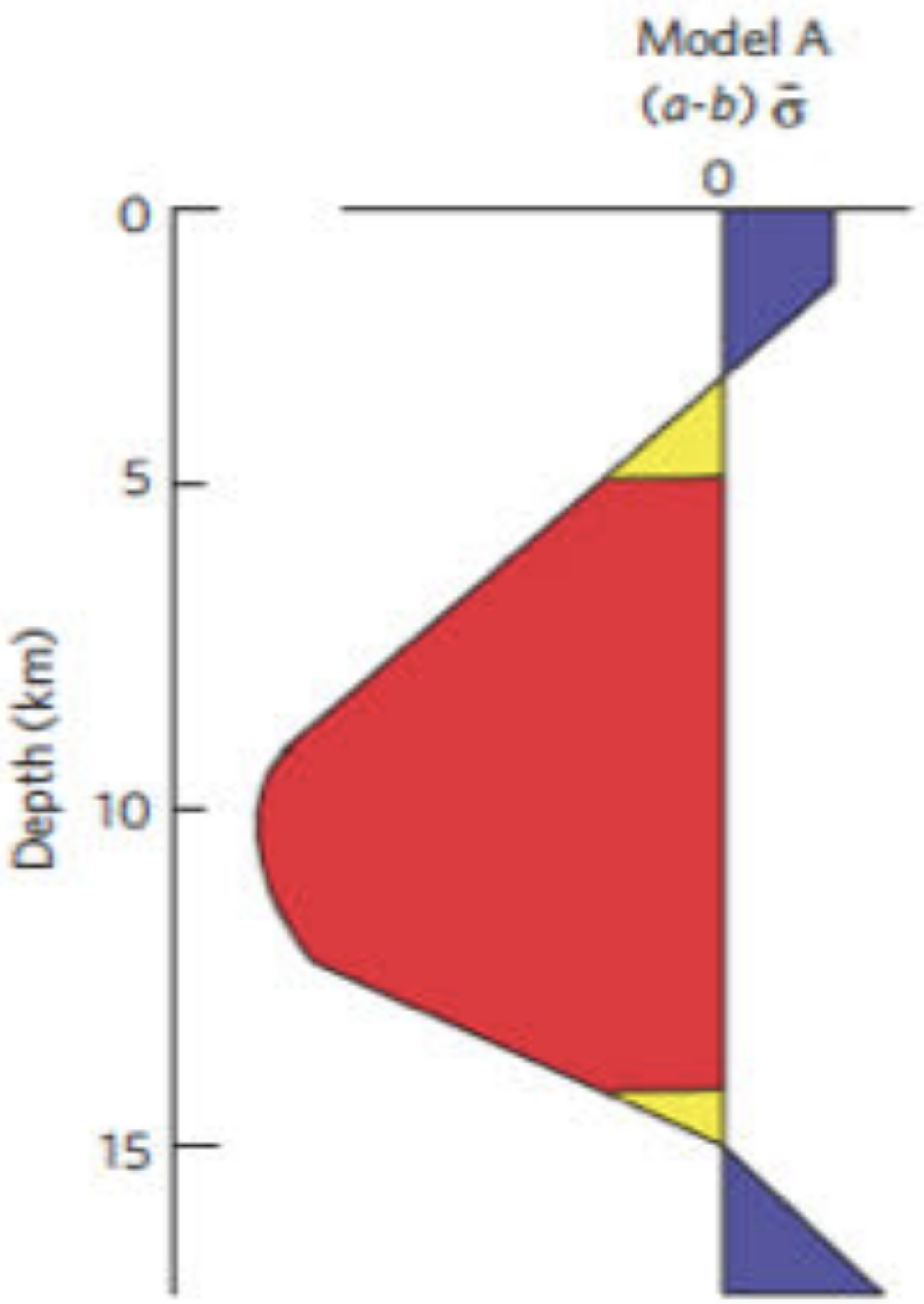

- **Apparently weak faults** due to combined effects of **severe velocity-weakening friction, elevated fluid pressure** and **fault geometry**

Note: seismogenic depth is here adapted by seismicity (Ross et al.2019)

- Fault friction: **rate-and-state friction with rapid velocity weakening** (Dunham et al., 2011) but statically 'strong' (0.6)

- Fault strength (fault local R-ratio) can be constrained **observationally** and with few **static calculations :**

$$R = \frac{\tau - \mu_d \sigma_n}{(\mu_s - \mu_d)\,\sigma_n} = \frac{\tau - f_w \sigma_n (1-\gamma)}{(f_0 - f_w)\sigma_n (1-\gamma)}$$

1. **Initial stress** (SH$_{max}$ here Andersonian + dCFS)

2. **Stress shape ratio** (balancing principal stress amplitudes)

3. **Fault strength of optimal oriented fault** (here: R0=0.8)

4. **Fluid pressure (here: elevated** but below hydrostatic, slightly decreased , i.e. higher stress drop, for the M7.1)

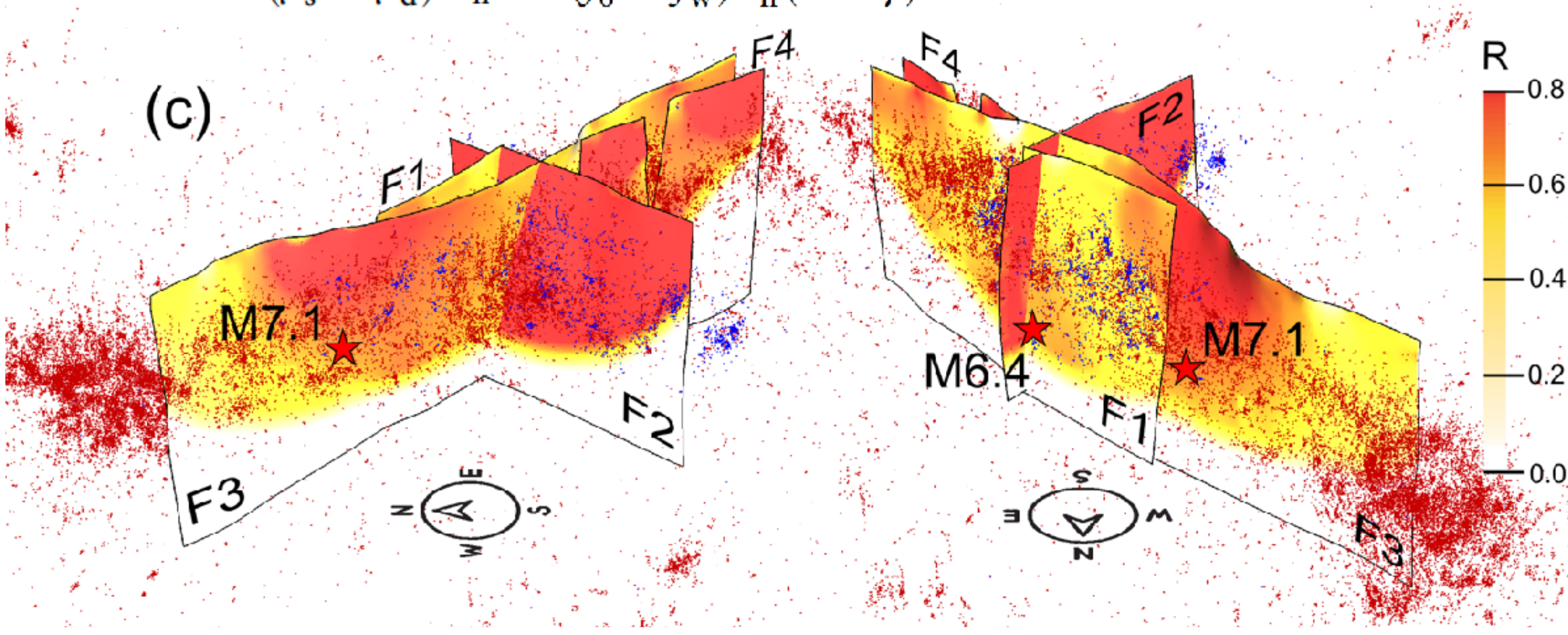

Using supercomputing (but not a lot of it)

- **Discretization:** ~10M elements, 200m spatial sampling of fault geometry, 200m finest sampling of topography
- **Resolution:** 2.4 elements per avg. process zone size 480m; seismic wavefield **up to 2 Hz** in fault vicinity
- **Off-fault plasticity:** Drucker-Prager elasto-viscoplastic rheology (Wollherr et al., 2018) **~10% overhead**
- Computational cost for both events: **6 hours** on **60 nodes** SuperMUC phase 2 ~ **9900 CPUh**

SuperMUC-NG - the 8th fastest supercomputer world-wide at the Leibniz Supercomputing Centre (LRZ)

Heinecke et al., Gordon Bell Prize Finalist, SC'14

Wollherr et al., JGR 2019

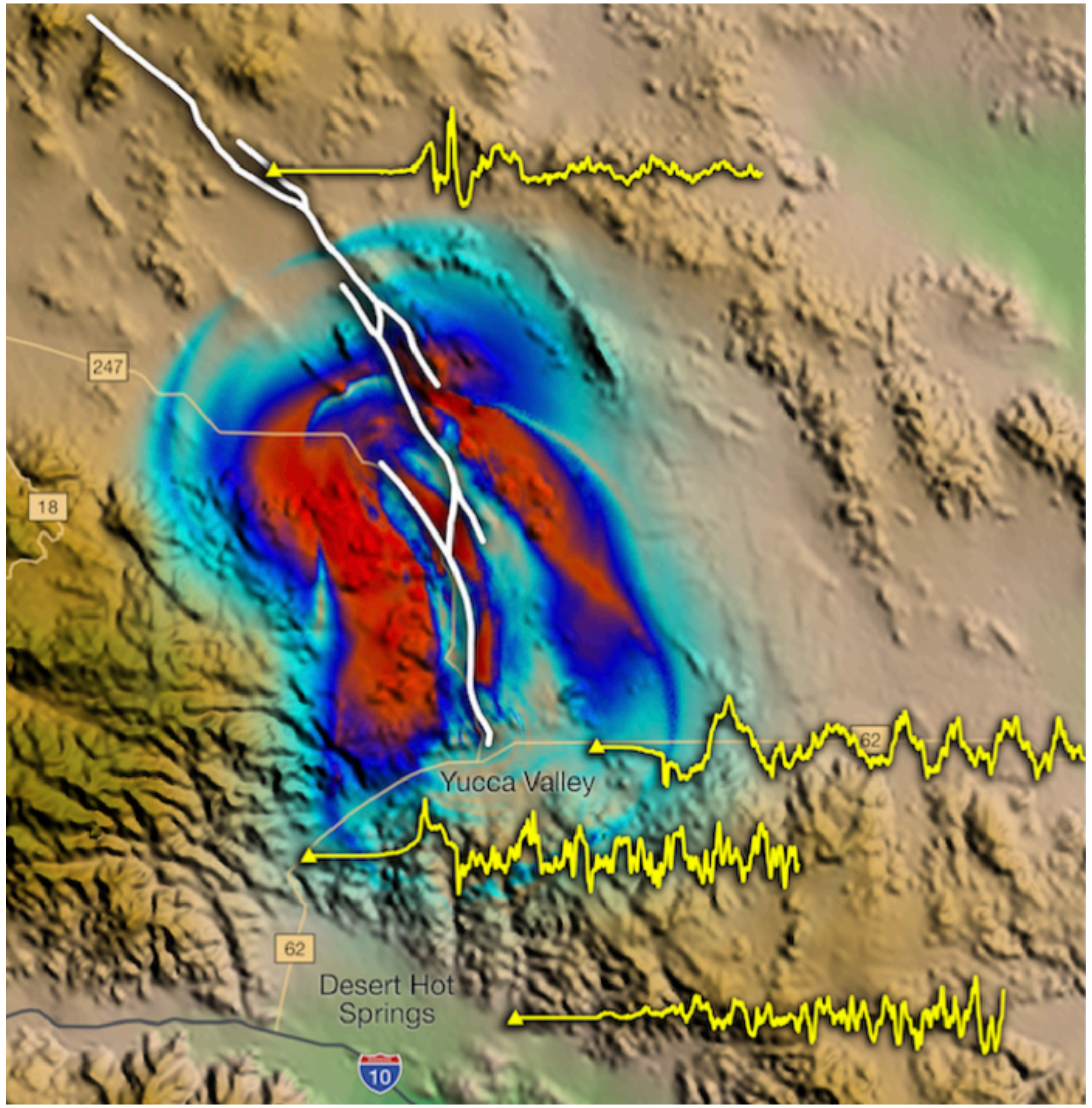

Landers earthquake dynamic rupture and 10 Hz wave propagation scenario (96 billion DoF, 200,000 time steps)

Coupled dynamic rupture scenario - the M6.4 Searles Valley event

- **Two conjugate faults rupture simultaneously** in the M6.4 scenario, while only the SW segment breaks the surface

max. slip F1: 2m F2: 1.5 m
average rupture velocity ~2.6 km/s
Mw ~6.54

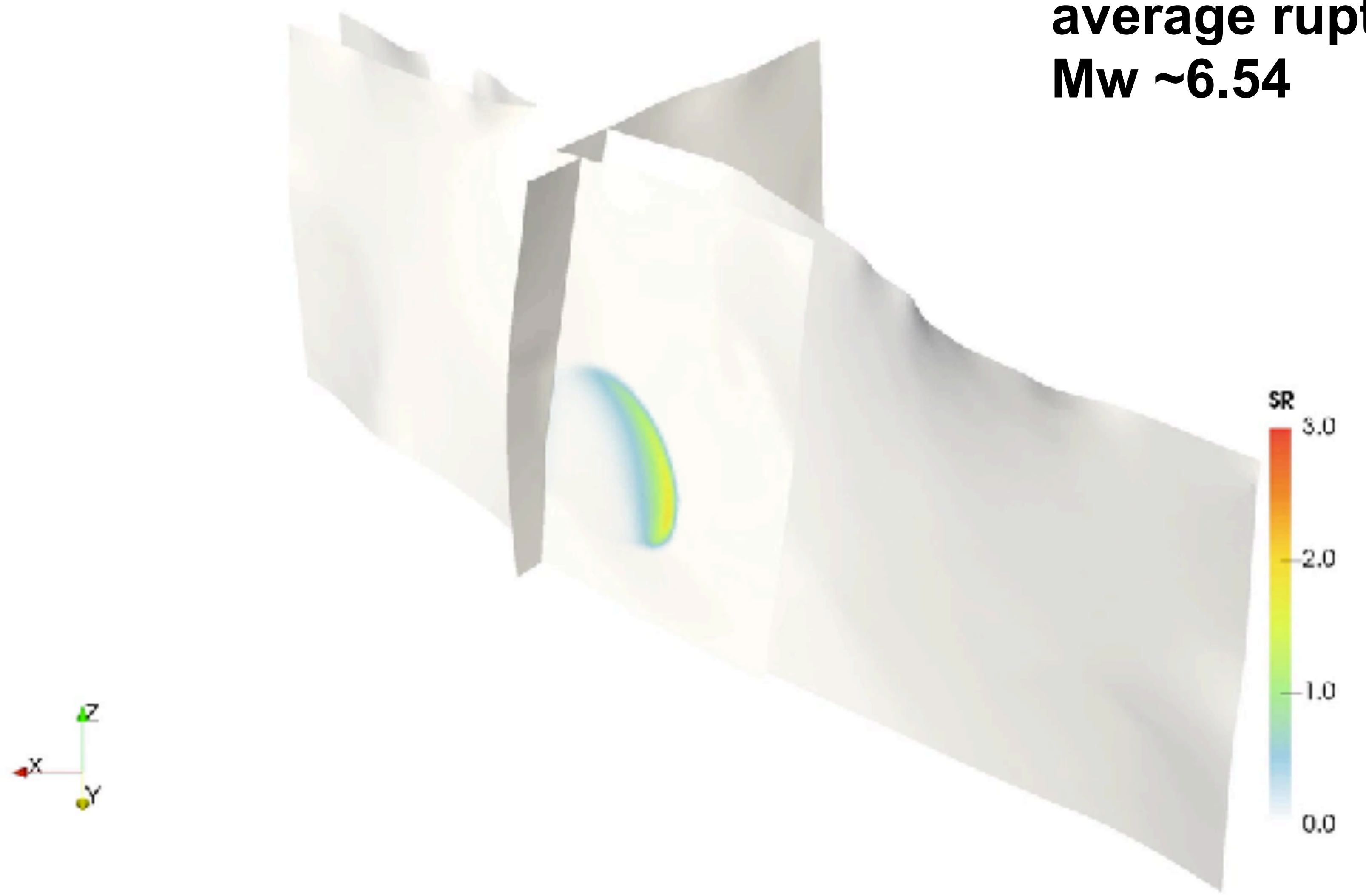

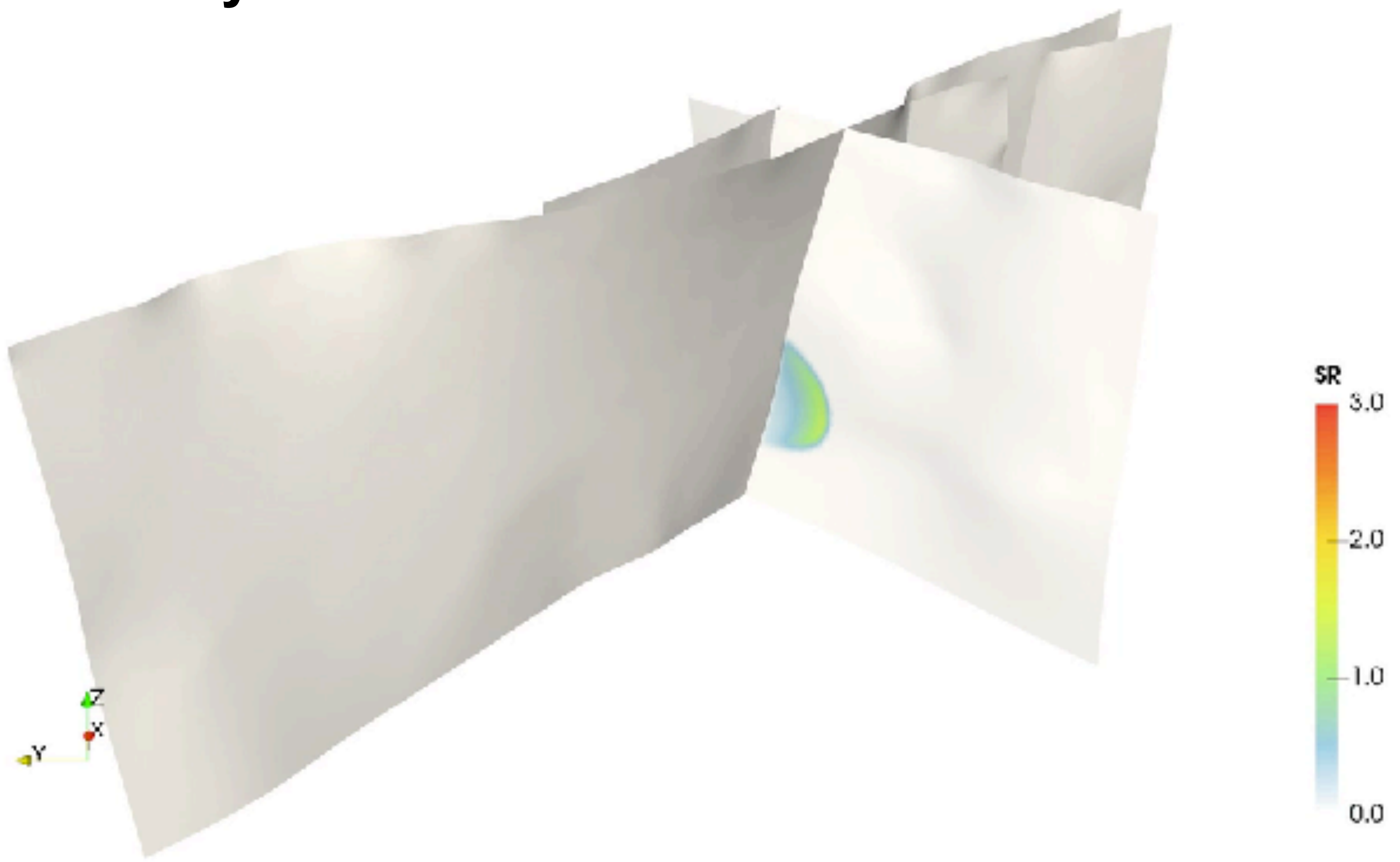

[Animation]

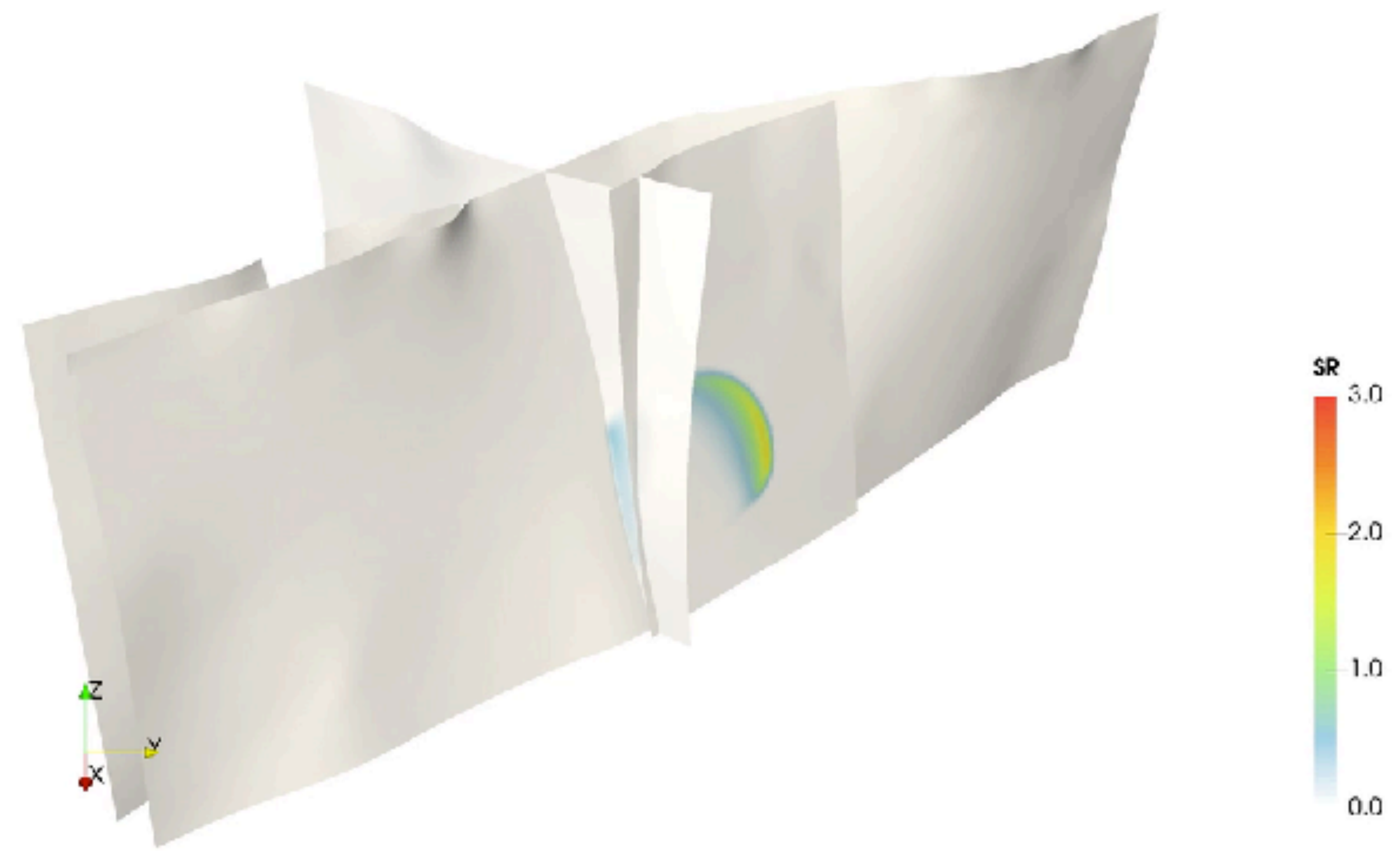

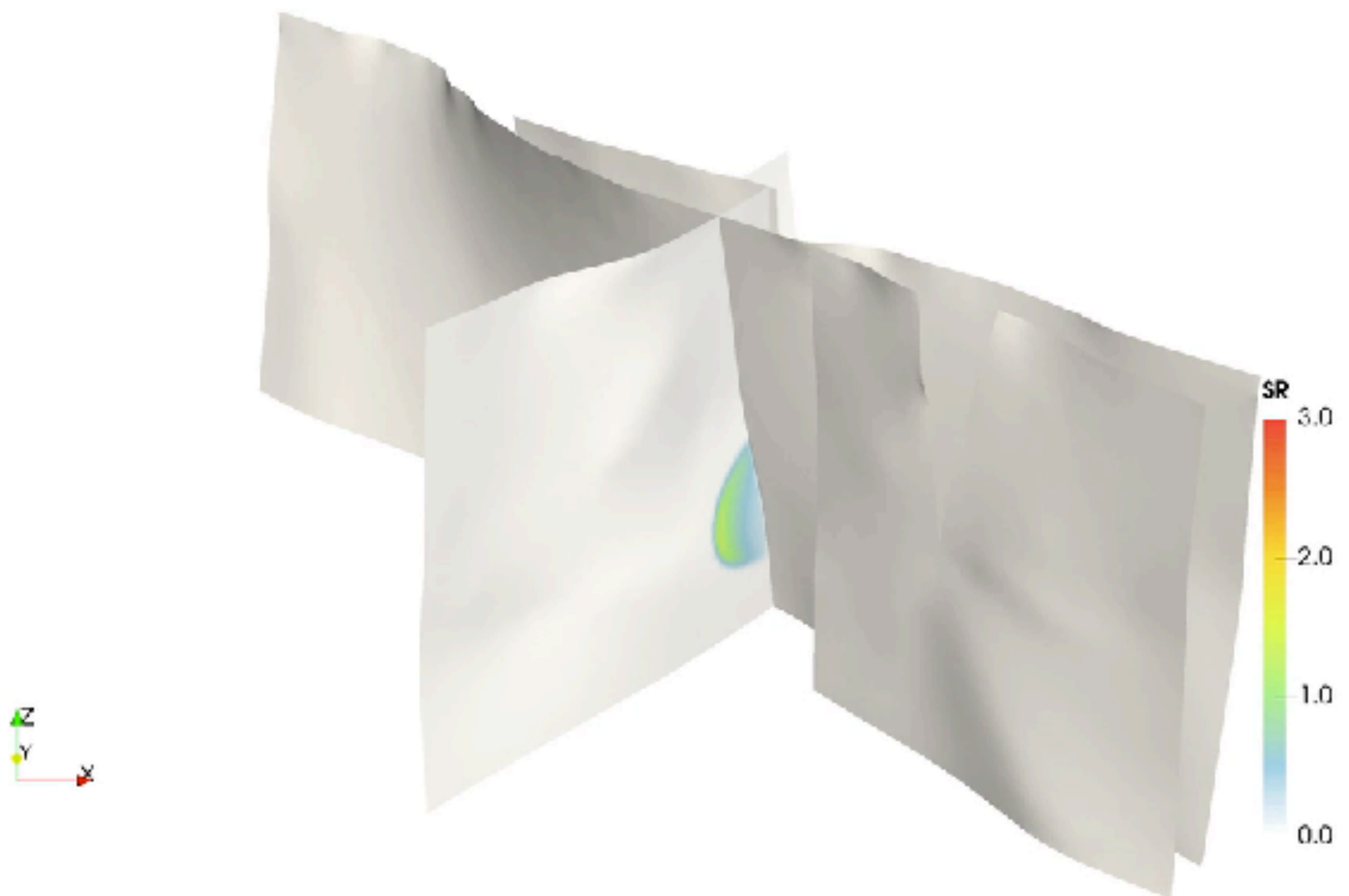

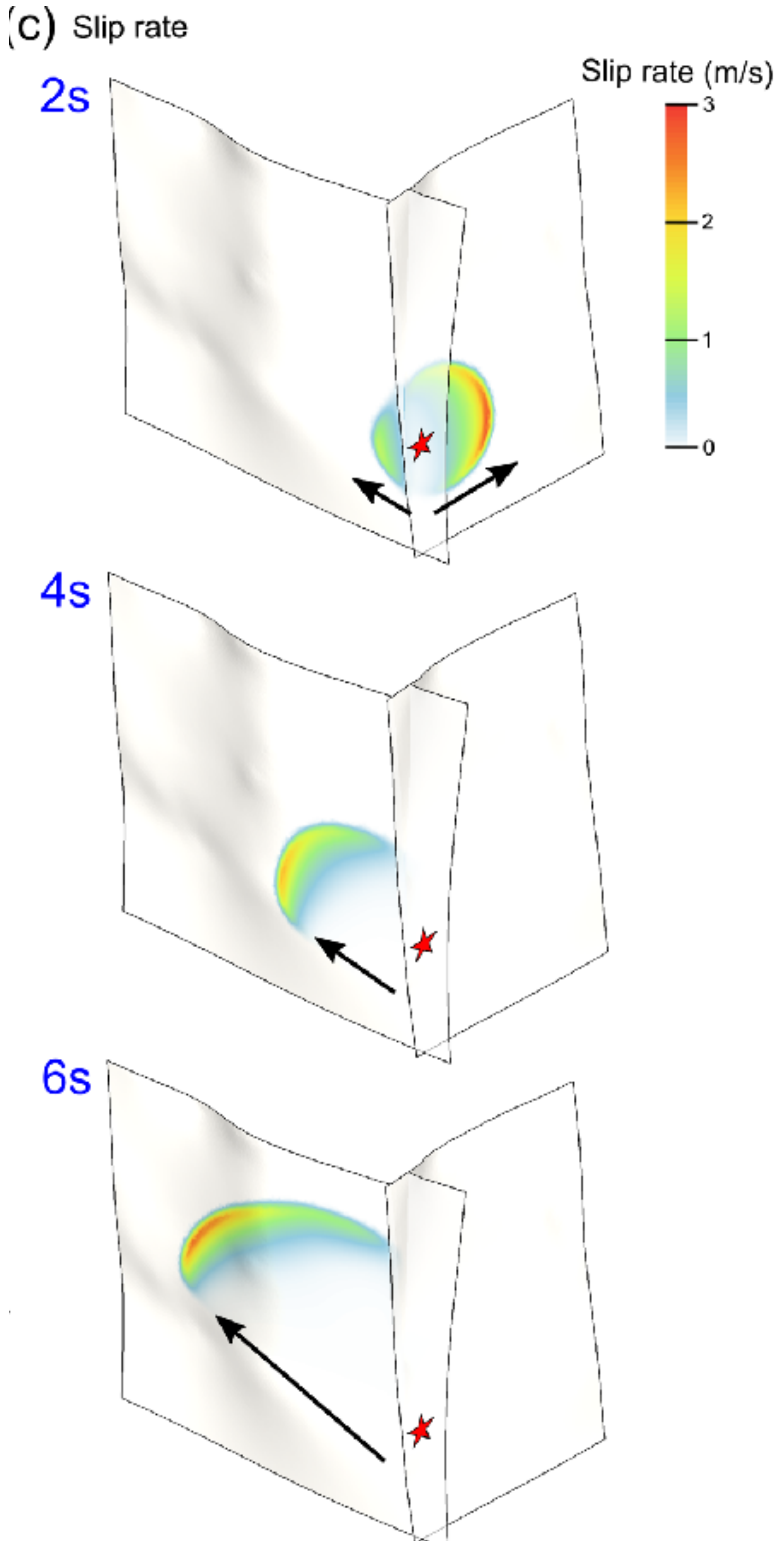

Coupled dynamic rupture scenario - the M6.4 Searles Valley event

- **Two conjugate faults rupture simultaneously** in the M6.4 scenario, while only the SW segment breaks the surface

max. slip F1: 2m F2: 1.5 m
average rupture velocity ~2.6 km/s
Mw ~6.44

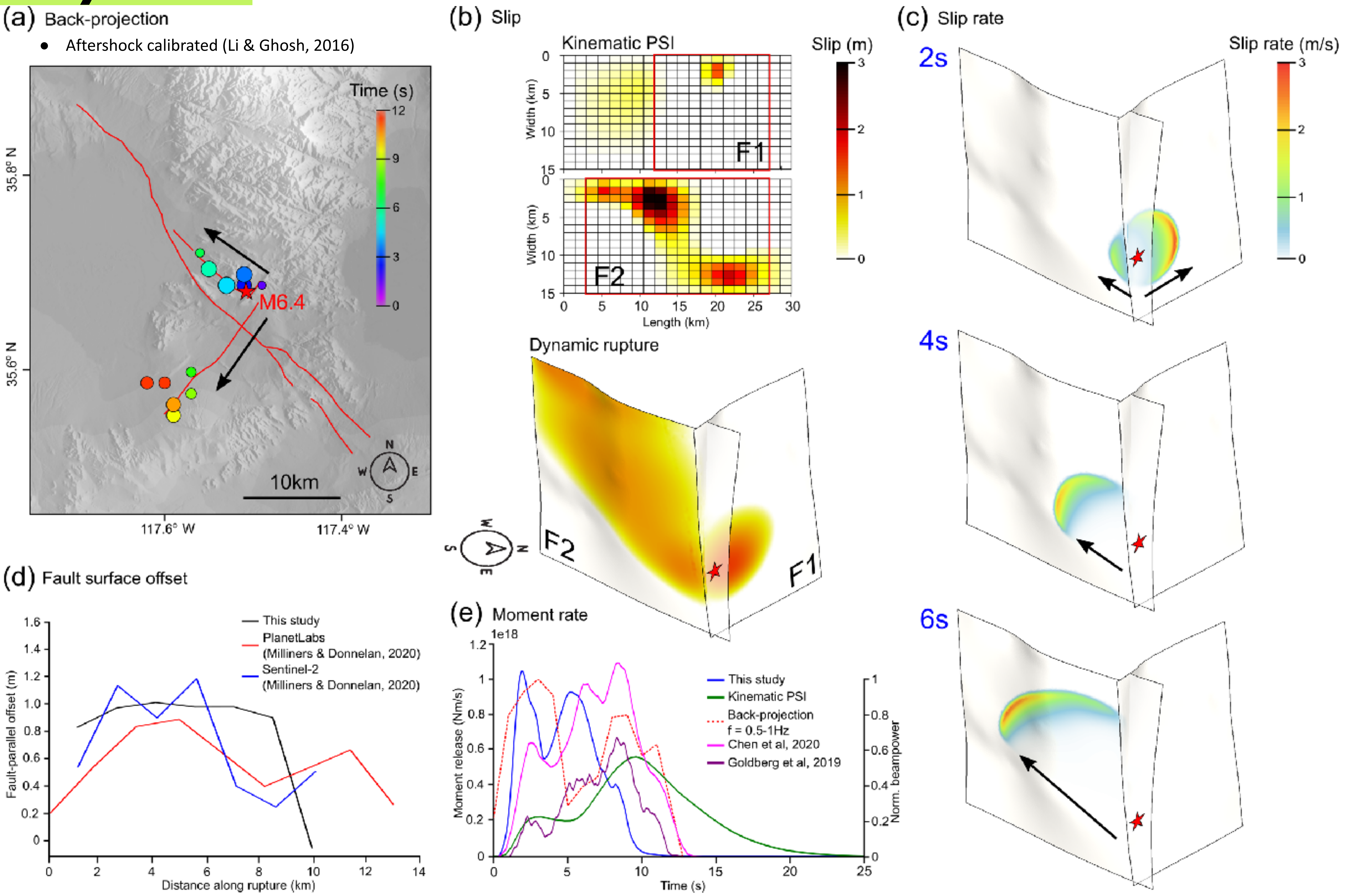

Coupled dynamic rupture scenario - the M6.4 Searles Valley event

- Good agreement in terms of ground deformation ground deformation compared to **InSAR, GPS and strong motion data** (given, that this is not an inversion)

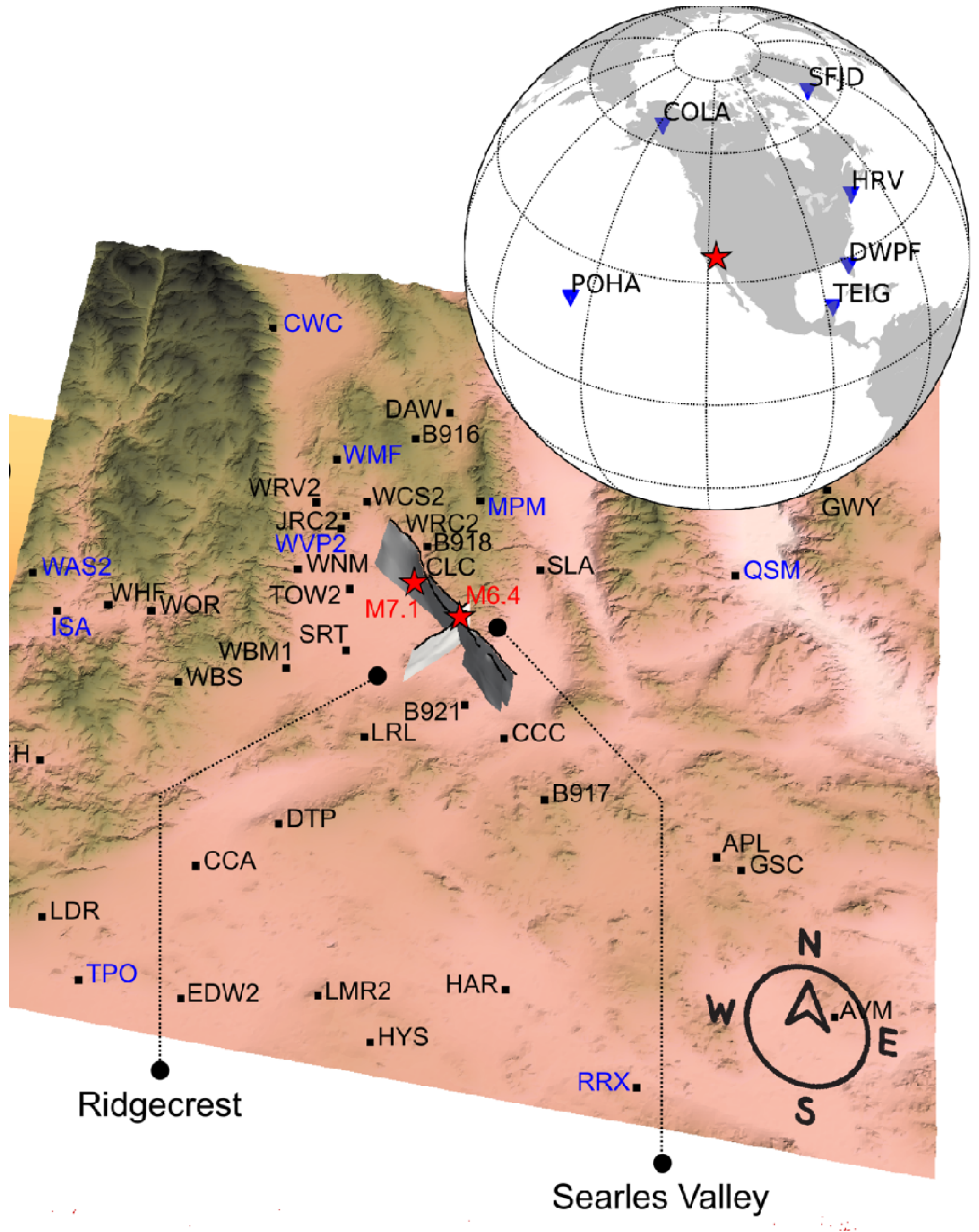

Comparison of synthetic **GPS** and observed detrended GPS vectors (UNAVCO: https://www.unavco.org). Colormap: synthetic slip on *Line of Sight* of **Sentinel-1 Descending Track T71** (Xu and Sandwell, 2019)

Comparison of synthetic (red) and observed (black) ground velocities, bandpass filtered: 0.1 - 0.5 Hz and 0.002 Hz - 0.02 Hz, time shifted, amplitude scaled

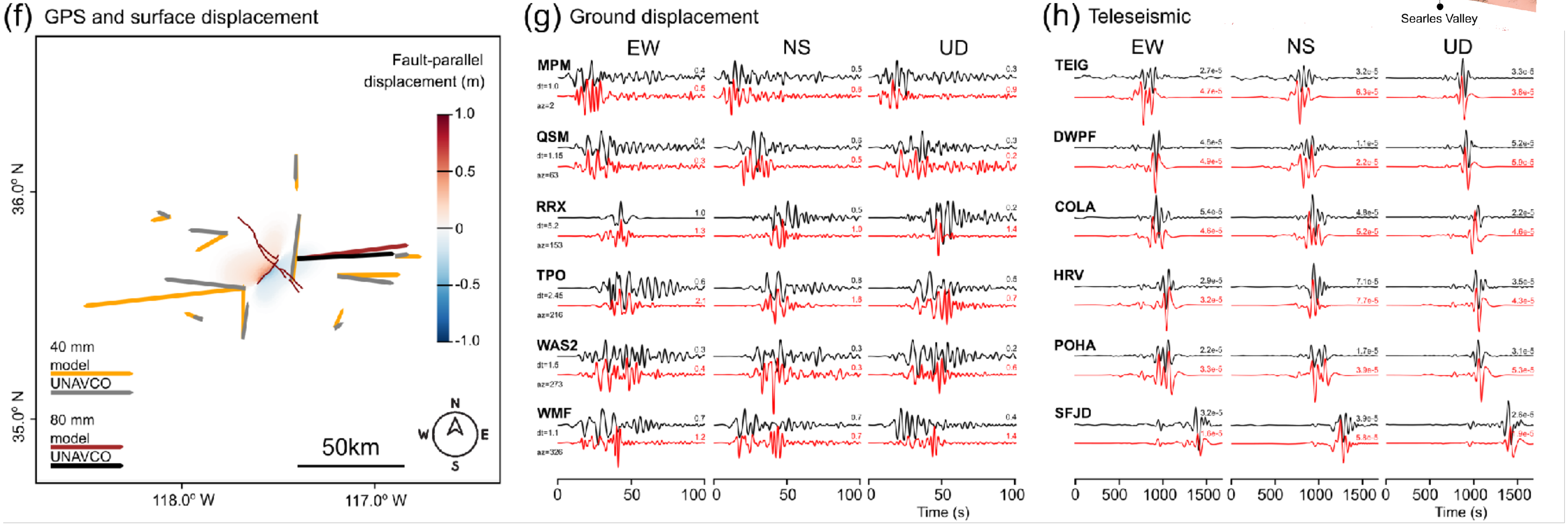

Coupled dynamic rupture scenario - the M6.4 Searles Valley event

- The M6.4 event causes a **CFS of about +0.25 MPa** at the SCEDC inferred hypocenter location of the M7.1, however, a considerate part of the main fault is 'shadowed' and hinders triggered rupture.

- The maximum dynamically transferred shear stress is 1.2 MPa during rupture of the M6.4

M6.4 Coulomb stress transfer calculated from our M6.4 scenario (see to the right) and assuming μ' = (1-γ)μ

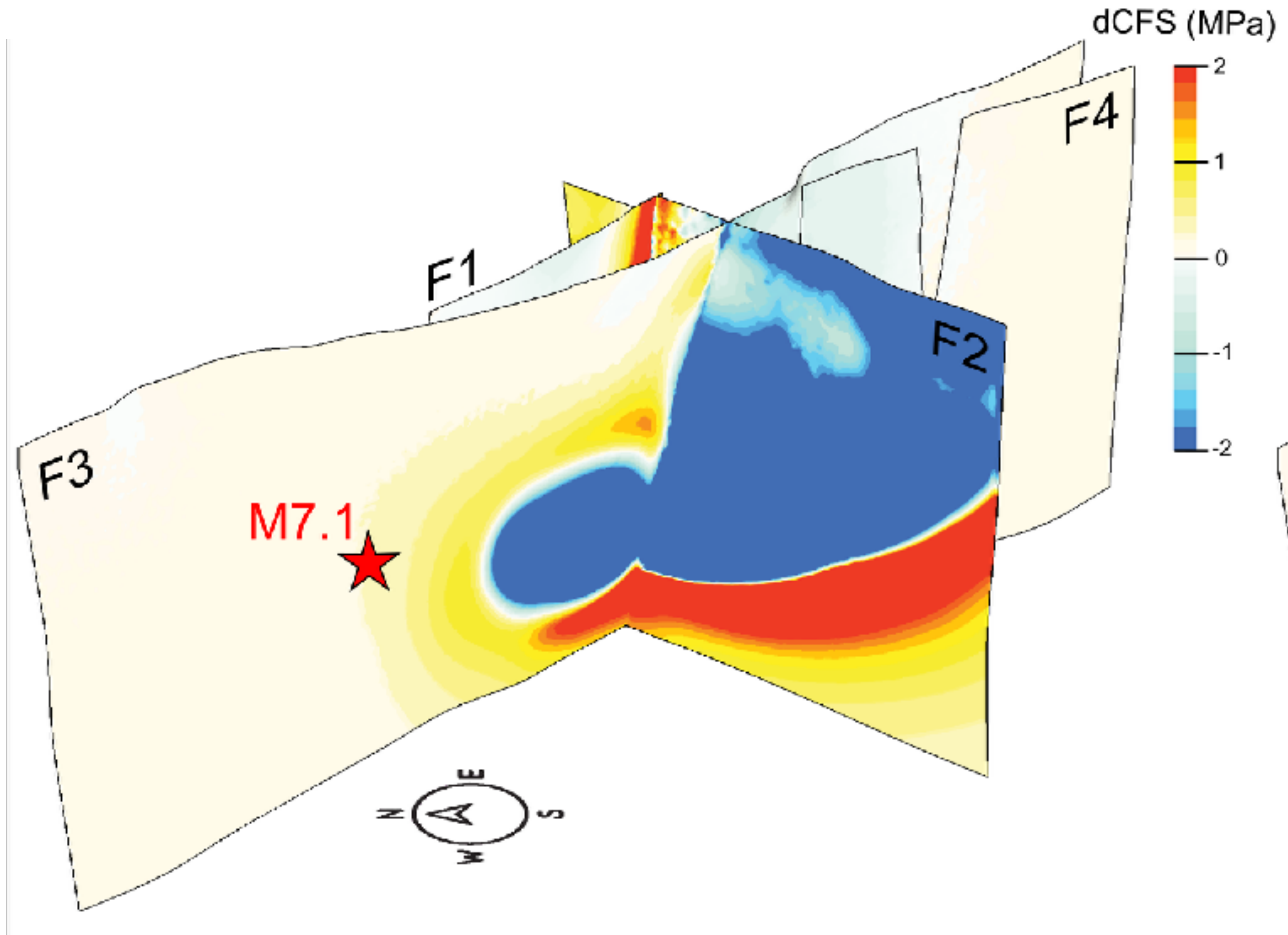

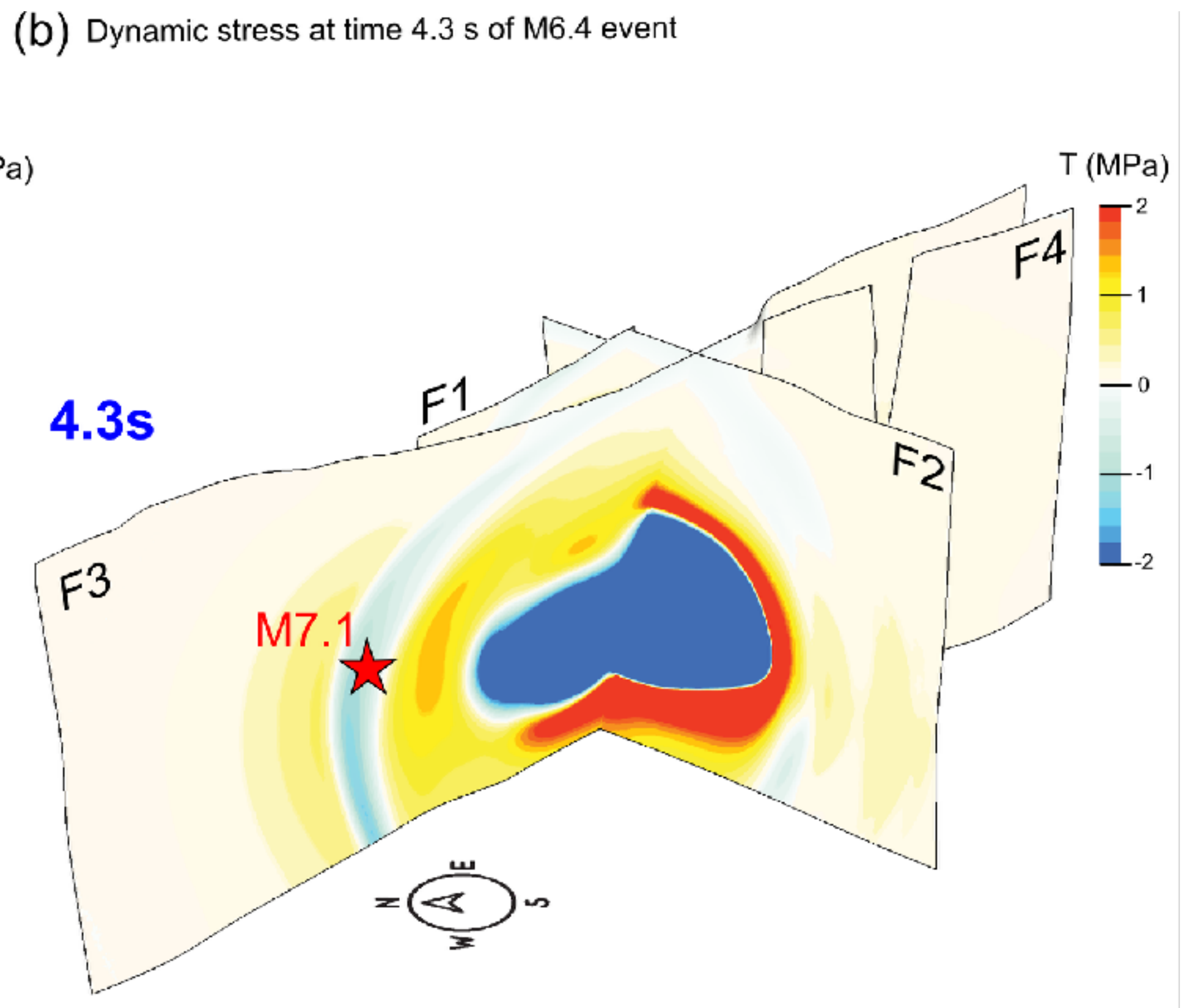

Coupled dynamic rupture scenario - the M7.1 Ridgecrest event

- Complex rupture including **re-activation of the SW segment** of the M6.4 conjugate fault and tunnelling beneath cross-section

M7.09
Max slip 3.8m

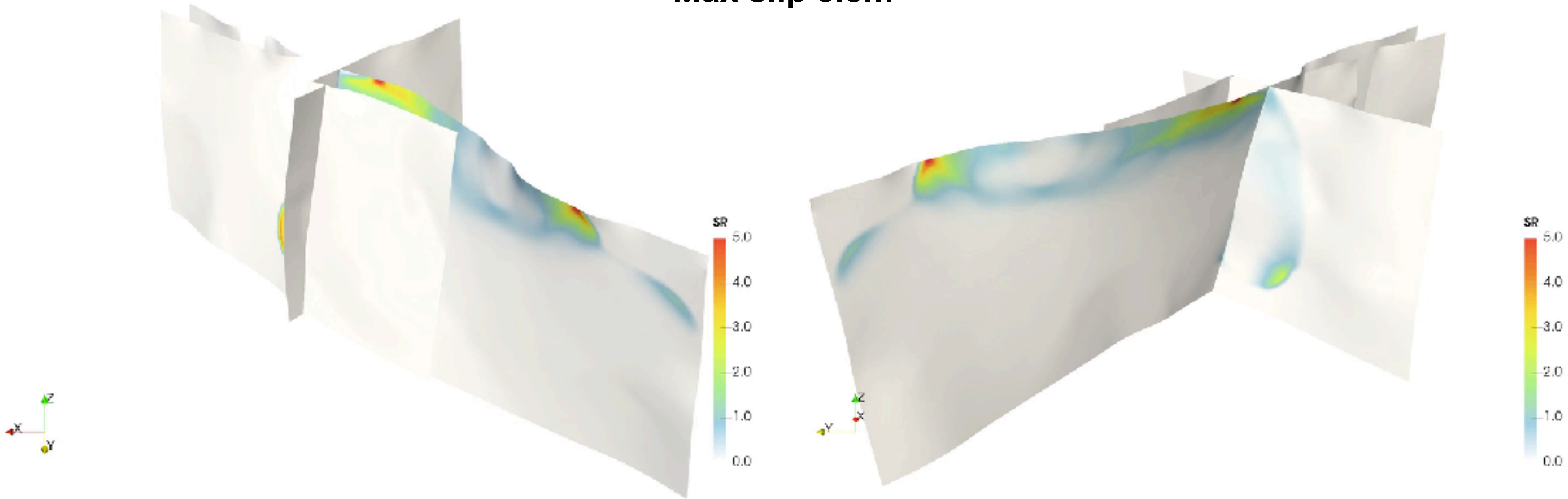

[Animation]

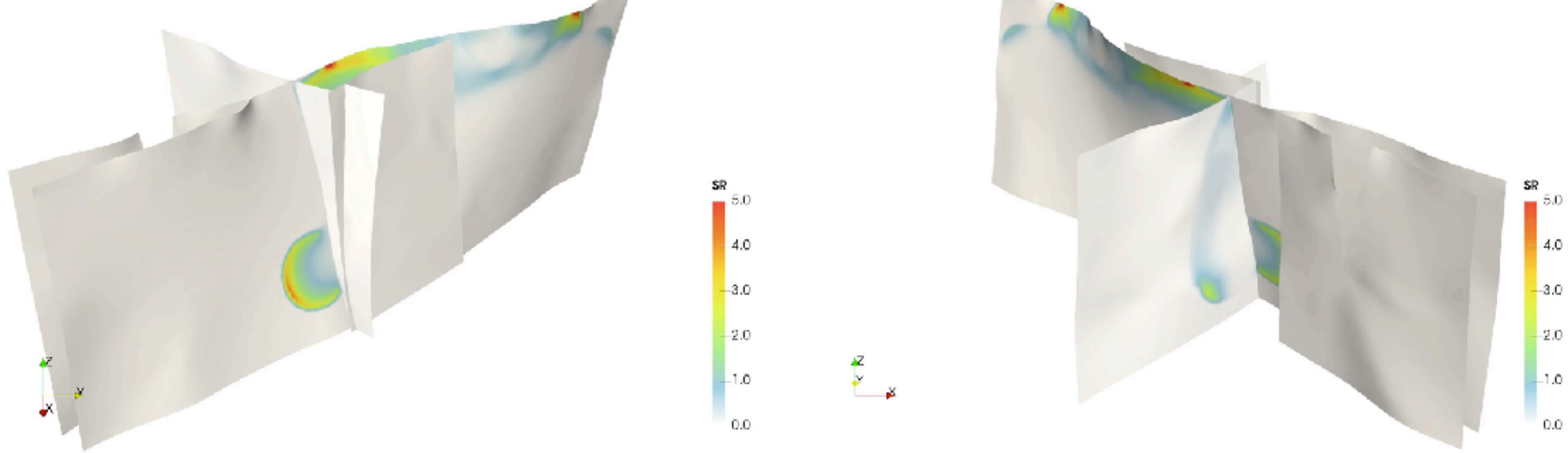

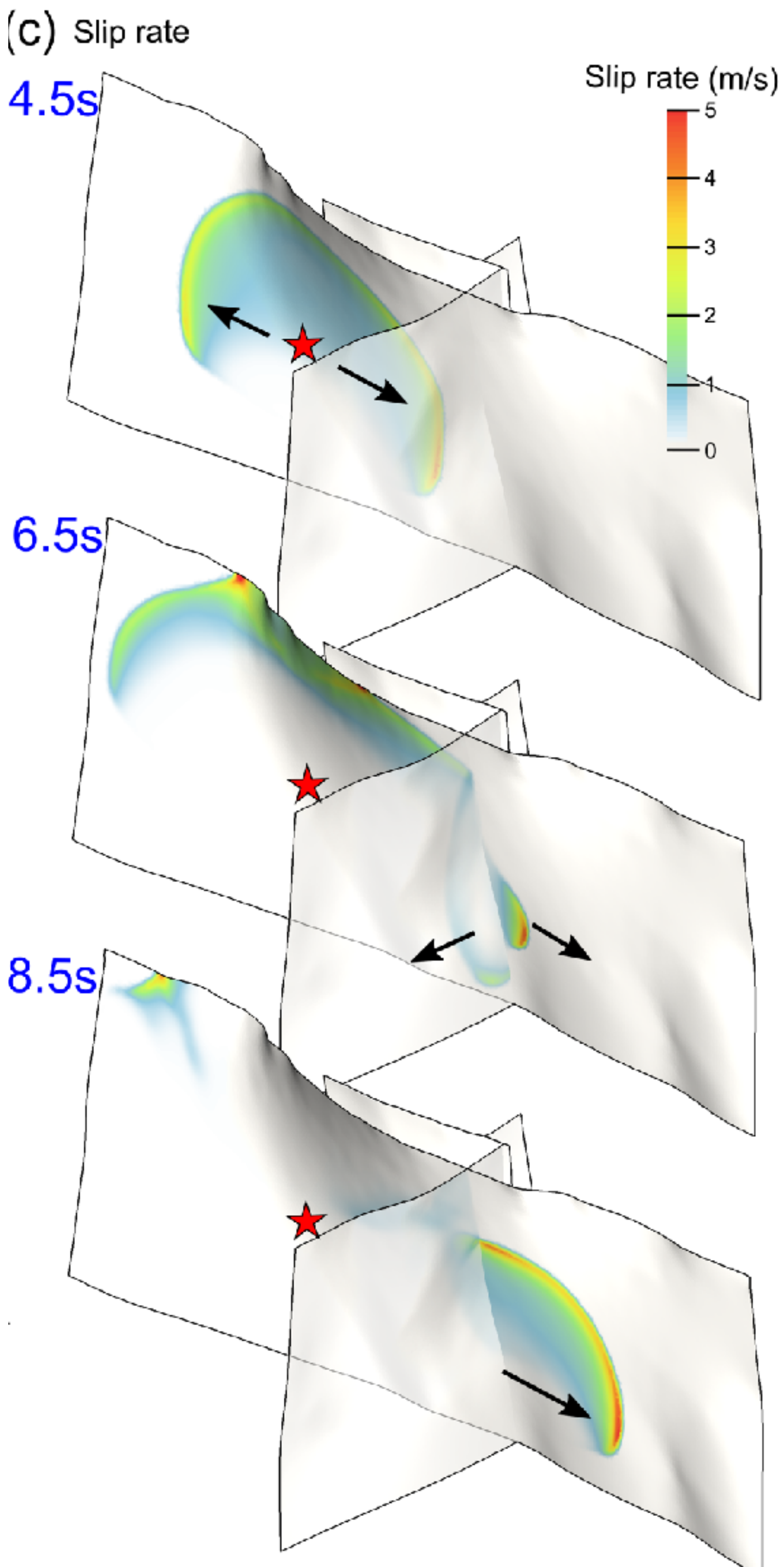

Coupled dynamic rupture scenario - the M7.1 Ridgecrest event

- Complex rupture including **re-activation of the SW segment** of the M6.4 conjugate fault and tunnelling beneath cross-section

M7.09
Max slip 3.8m
Too fast average rupture velocity ~2.65 (North) -2.95 km/s (South)
cf. BP only 2.5 km/s

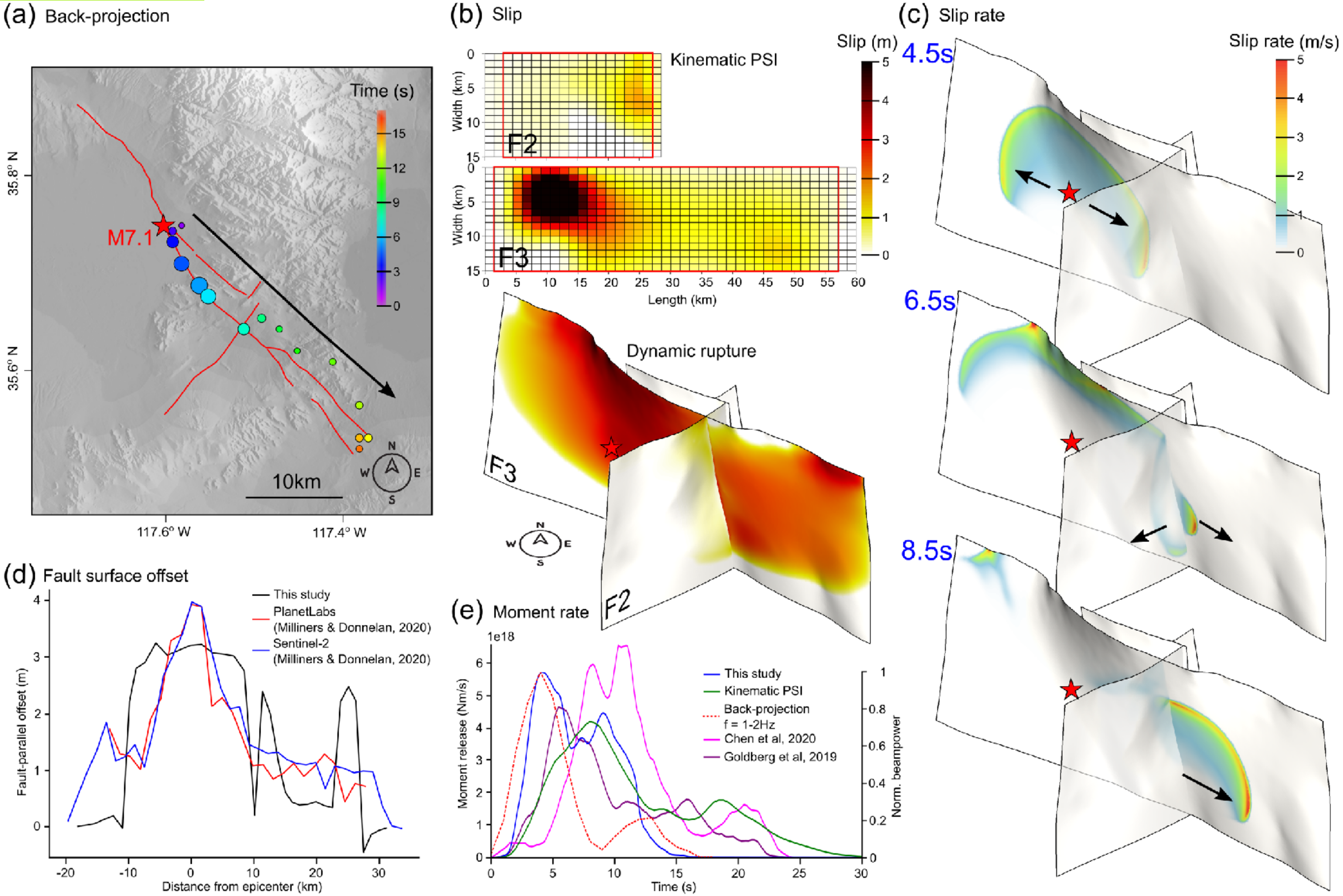

Coupled dynamic rupture scenario - the M7.1 Ridgecrest event

- Good agreement in terms of ground deformation ground deformation compared to **InSAR, GPS and strong motion data** (given, that this is not an inversion)

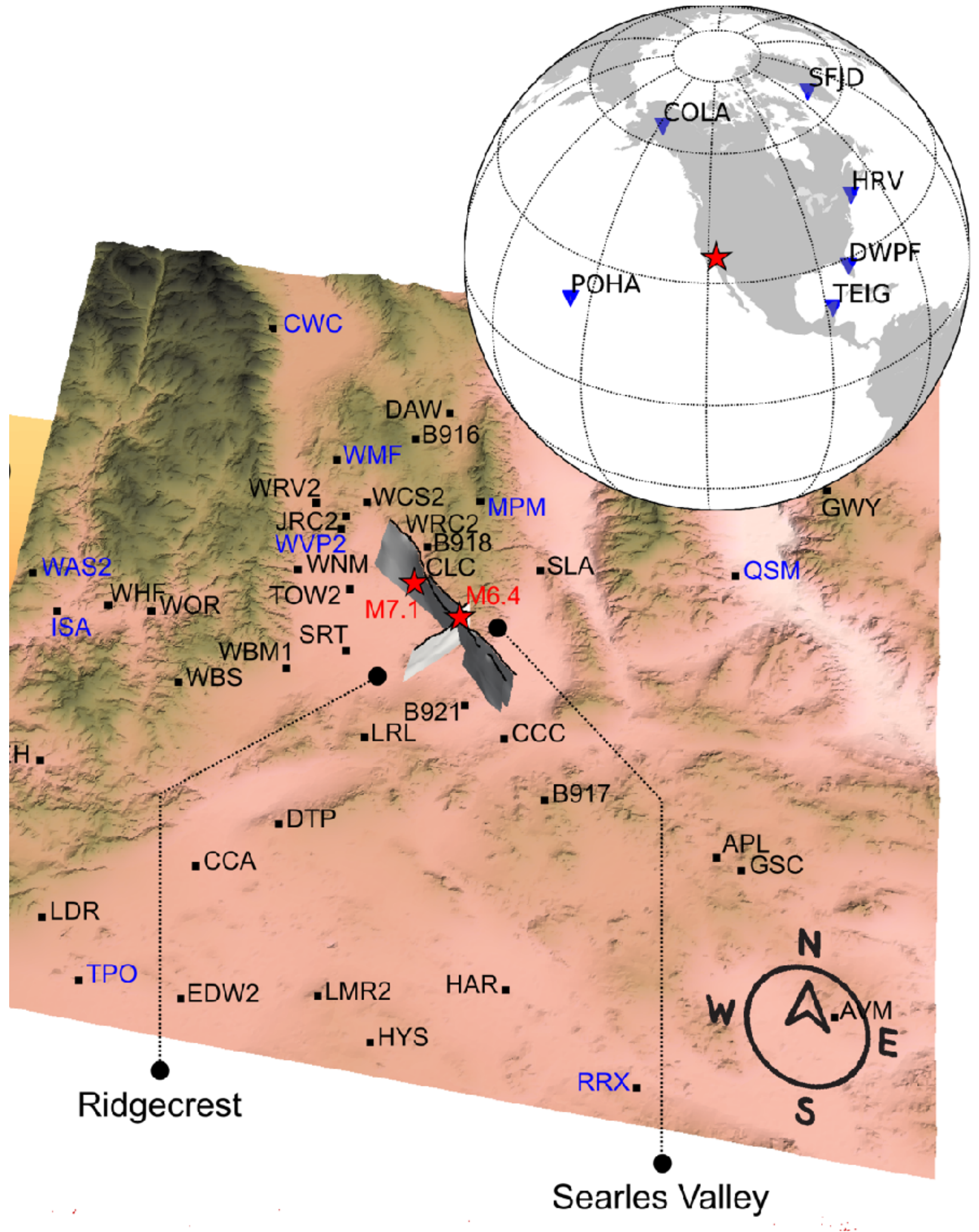

Comparison of synthetic **GPS** and observed detrended GPS vectors (UNAVCO: https://www.unavco.org). Colormap: synthetic slip on *Line of Sight* of **Sentinel-1 Descending Track T71** (Xu and Sandwell, 2019)

Comparison of synthetic (red) and observed (black) ground velocities, bandpass filtered: 0.1 - 0.5 Hz and 0.002 Hz - 0.02 Hz, time shifted, amplitude scaled

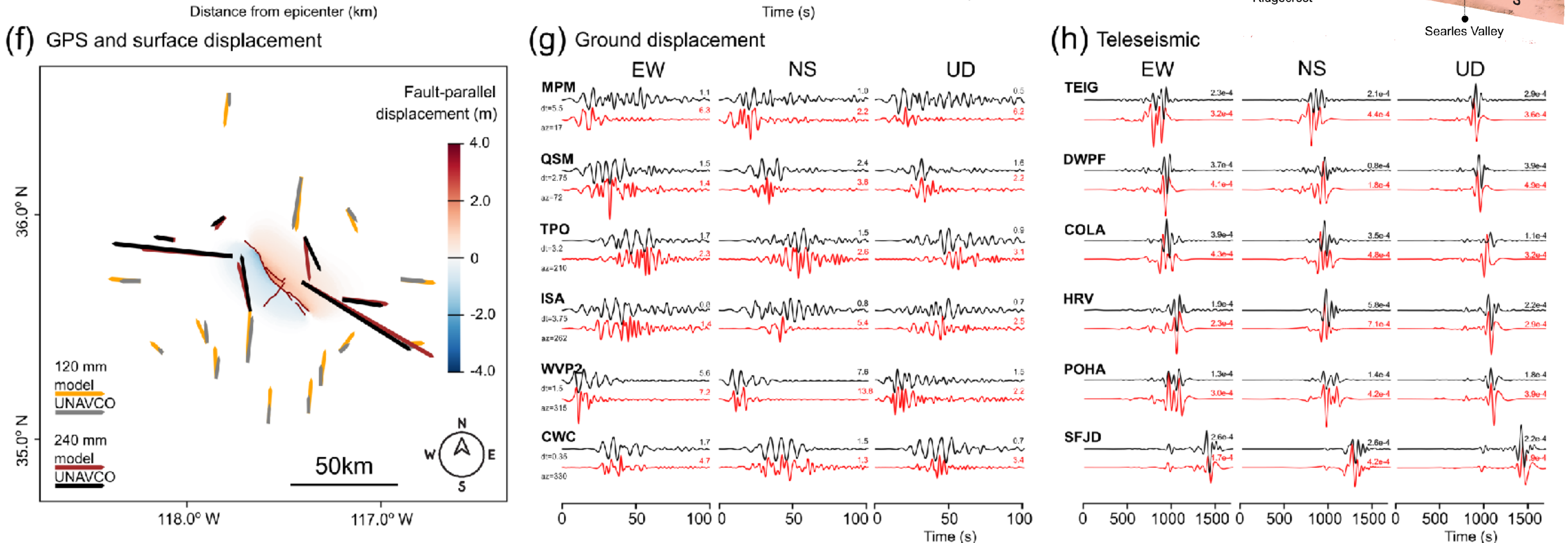

Coupled dynamic rupture scenario - off-fault damage

- **Drastic increase** of **off-fault deformation** in **geometrically complex fault regions** enhancing geometric barriers, hindering rupture transfers and matching fault zone width mapping

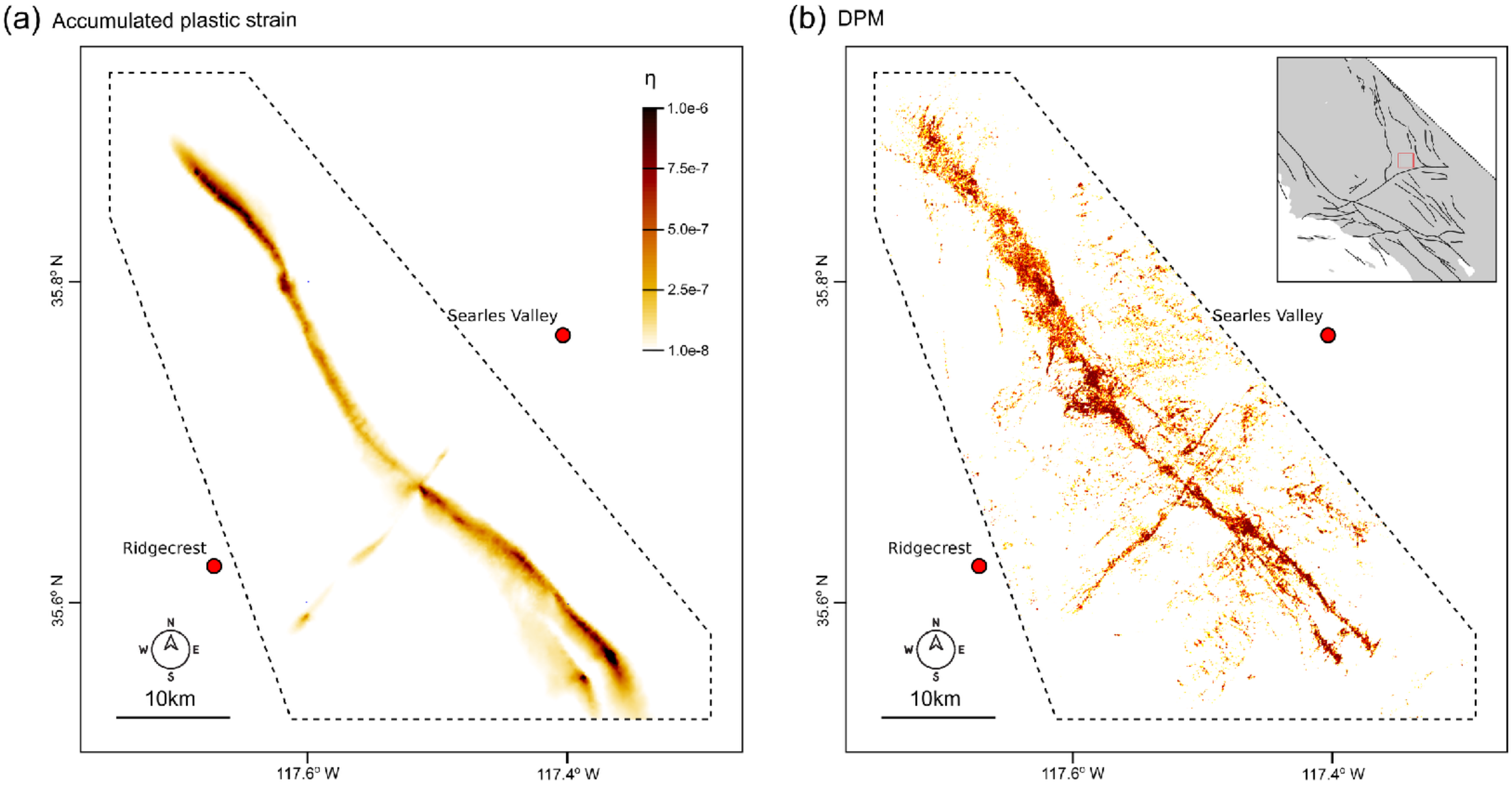

Outlook

- Synthetic data, e.g. at lines of sensors crossing the rupture, can illustrate the **richness** of results **extreme near-field** observations may provide

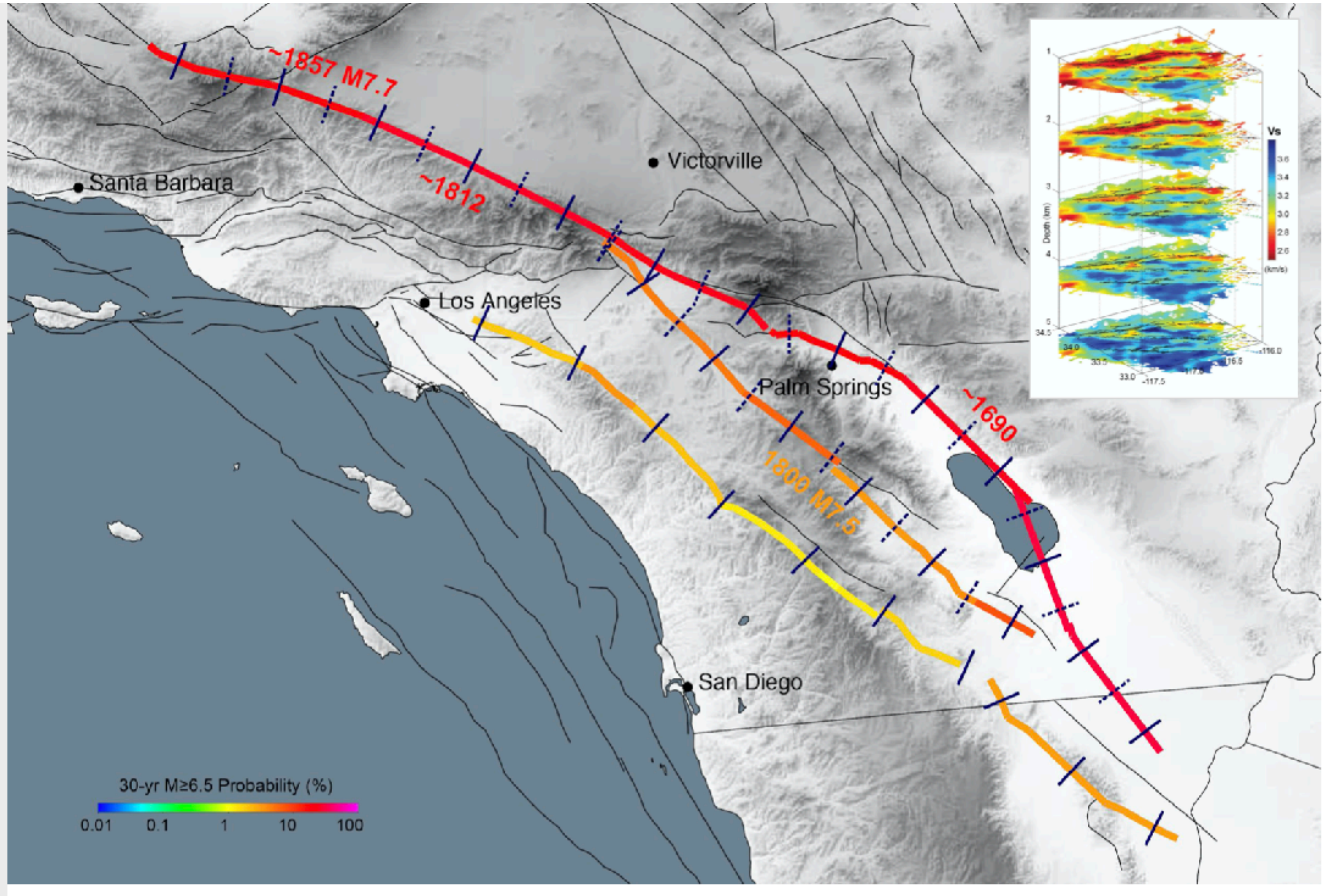

A proposed RUPTURE and FAULT ZONE OBSERVATORY (courtesy of Y. Ben-Zion) consisting of linear arrays of sensors across the major faults in southern California every 20-30 km to provide unprecedented in situ recording of dynamic fields within rupture zones.

Outlook

- Synthetic data, e.g. at lines of sensors crossing the rupture, can illustrate the **richness** of results **extreme near-field** observations may provide

- Synthetic near-field ground motions may help us to identify what to look for, e.g., in the vast amount of DAS data

- Approx. **near-field corner frequencies** of **100k synthetic spectra** (up to 2 Hz) with high variability in corner frequencies

- **Rays of elevated corner frequencies** in vertical components radiating from each slipping fault at 45 degree

- **Direct body waves** depending on take-off angle and directivity effects which enriched in high-frequencies (cf. Kaneko & Shearer, 2014)

- Potential for inferring stress drop, focal mechanisms, rupture segmentation from **near-field data**

The 1992 Mw 7.3 Landers earthquake "reloaded"
(Wollherr, 2019; Schliwa and Gabriel, EGU Display D1781)

Synthetic corner frequencies of vertical ground motion spectra

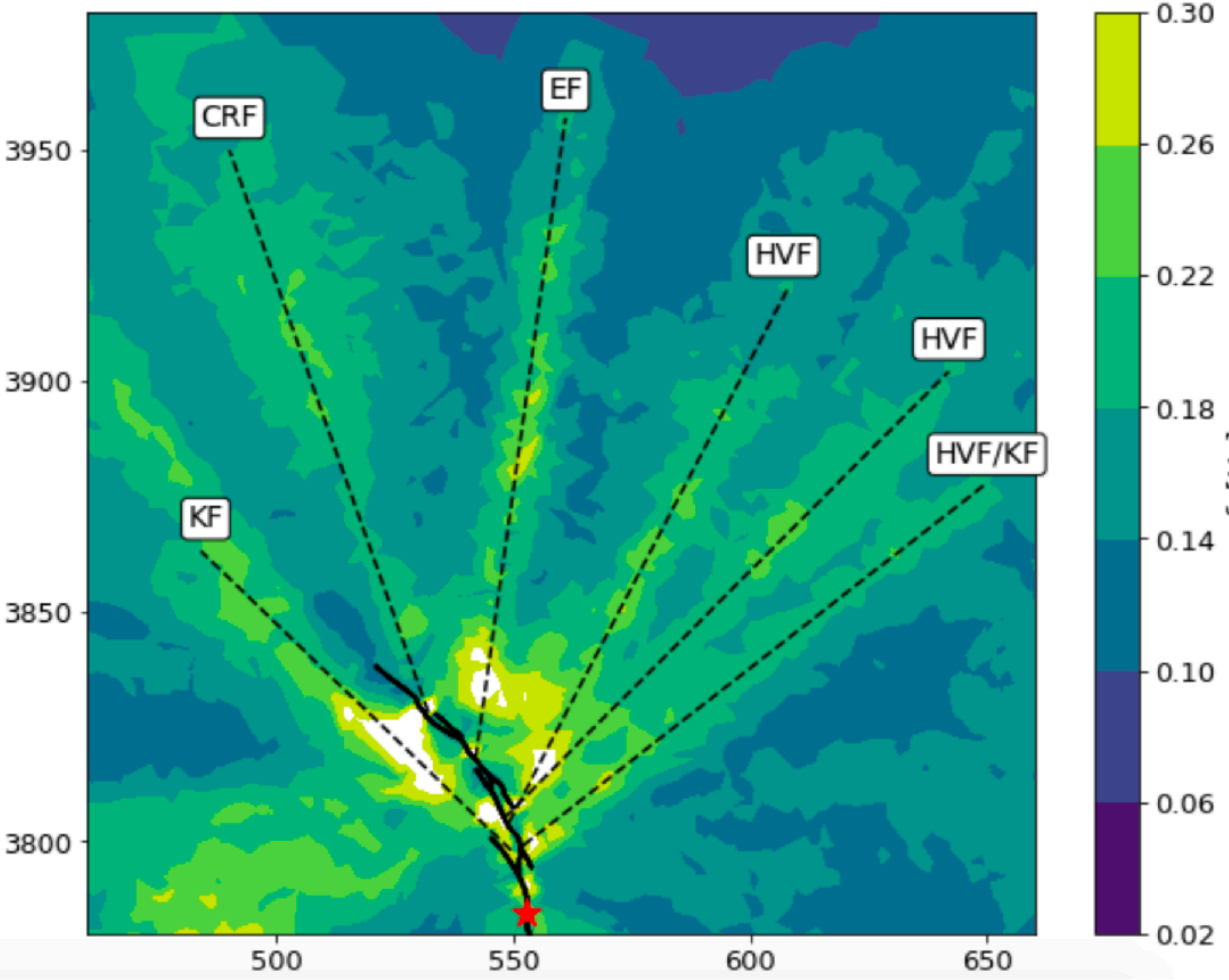

cf. The corner frequency shift, earthquake source models and Q, T.C. Hanks, 1980

Summary:

- Combined dynamic rupture scenarios of the 2019 Searles Valley and Ridgecrest sequence can be constrained and validated by observations
- These show a high sensitivity to the 3D stress state, specifically in the vicinity of complexities in fault geometry
- Two conjugate faults rupture simultaneously in the M6.4 and the M7.1 re-ruptures the SW segment of the conjugate fault. The M6.4 induces considerable Coulomb and dynamic stress changes in the Mw7.1 hypocentral region; however, not enough to trigger rupture across the stress-shadowed main fault.
- Both scenarios match key observations including magnitude, directivity, off-fault damage, slip distribution from kinematic inversion, teleseismic waveforms, GPS, and InSAR ground deformation
- The match with seismic and geodetic data is surprisingly fair (given this is not an inversion), however we may be missing near-fault zone properties, specifically to capture rupture speed

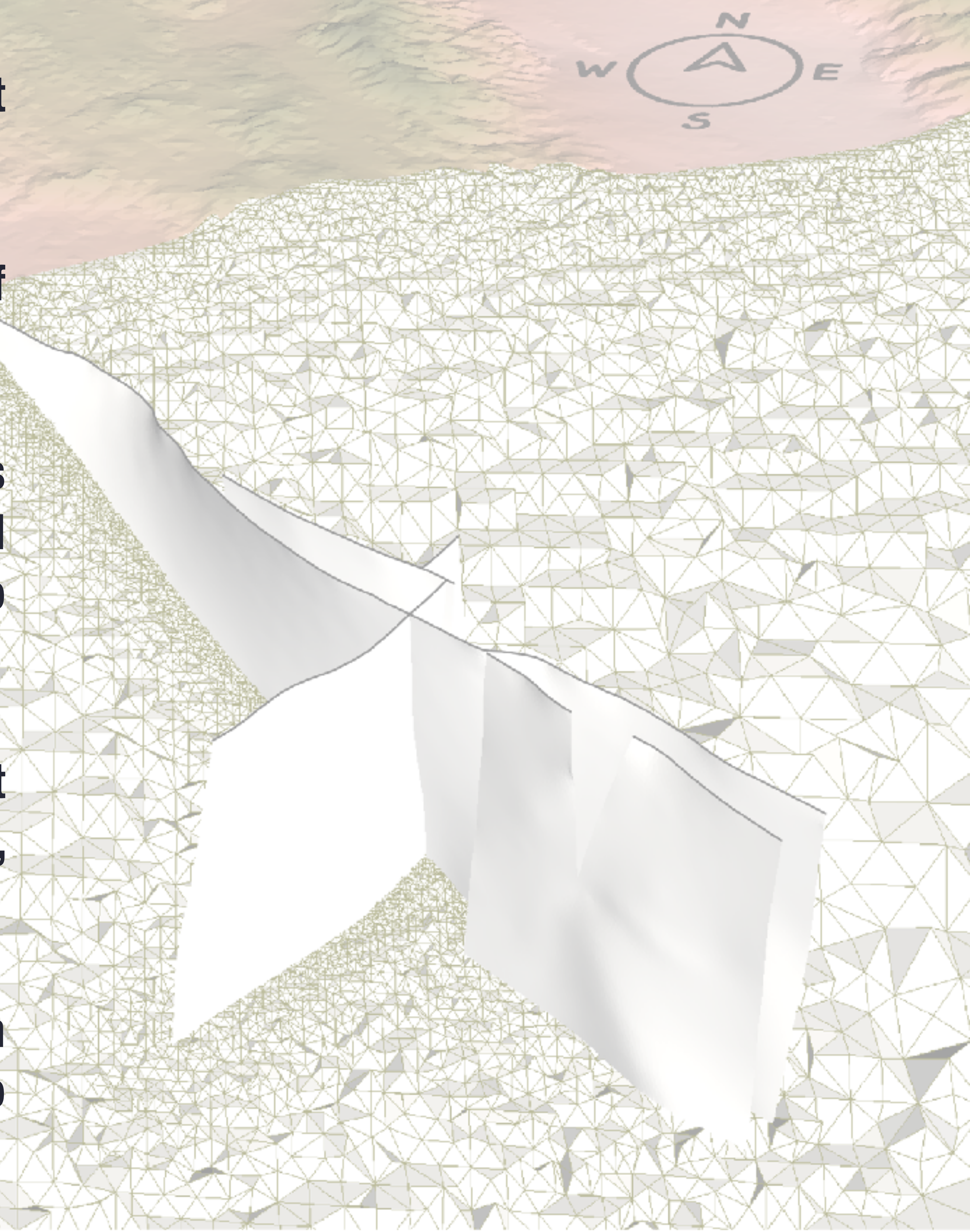

Summary:

- Physics-based modeling provides mechanically viable insight into the physical conditions that allow rupture on complex fault systems and helps constraining competing views on earthquake sources

- Observational constraints, specifically community models, can be routinely included; Observational methods can themselves be constrained

- Advances in high-performance computing and dense observations allow us to go beyond scenario-based analysis, aiming for urgent response quickly after an event occurs, ensemble simulations, dynamic inversion and uncertainty quantification